# Chapter 2
# Patterns of Embryonic Development in Early to Middle Devonian Ammonoids

**Susan M. Klofak,[1] Neil H. Landman,[2] and Royal H. Mapes[3]**

[1]Division of Paleontology (Invertebrates), American Museum of Natural History, 79th Street and Central Park West, New York, NY 10024, USA, and Department of Biology, City College of the City University of New York, Convent Avenue and 138th Street, New York, NY, 10031, USA, klofak@amnh.org;

[2]Division of Paleontology (Invertebrates), American Museum of Natural History, 79th Street and Central Park West, New York, NY 10024, USA, landman@amnh.org;

[3]Department of Geological Sciences, 316 Clippinger Laboratories, Ohio University, Athens, OH 45701–2979, USA, mapes@ohio.edu



**Keywords:** Devonian, ammonitella, Agoniatitidae, Mimagoniatitidae, Anarcestidae, New York, Morocco

## 1 Introduction

The basic structure of the ammonitella or embryonic shell of the Ammonoidea has been well documented (Sandberger, 1851; Branco, 1879–1880, 1880–1881; Schindewolf, 1933; Erben, 1960). The ammonitella begins with a small egg-shaped or spherical initial chamber (=protoconch) (for discussion of terms see Schindewolf, 1933; House, 1996; and Landman et al., 1996; see Landman et al., 1996 for additional references) and extends as a straight shaft or coiled tube (called the ammonitella coil by House, 1996: 168). In most species the ammonitella extends approximately one whorl ending in a primary constriction (Landman et al., 1996; Klofak et al., 1999). Internally, the siphuncle originates in the initial chamber as a rounded caecum and is attached to the shell wall by a prosiphon (Landman, 1988: Figs. 1, 2 and Klofak et al., 1999: Figs. 1, 2).



N. H. Landman et al. (eds.), *Cephalopods Present and Past: New Insights and Fresh Perspectives*, 15–56.

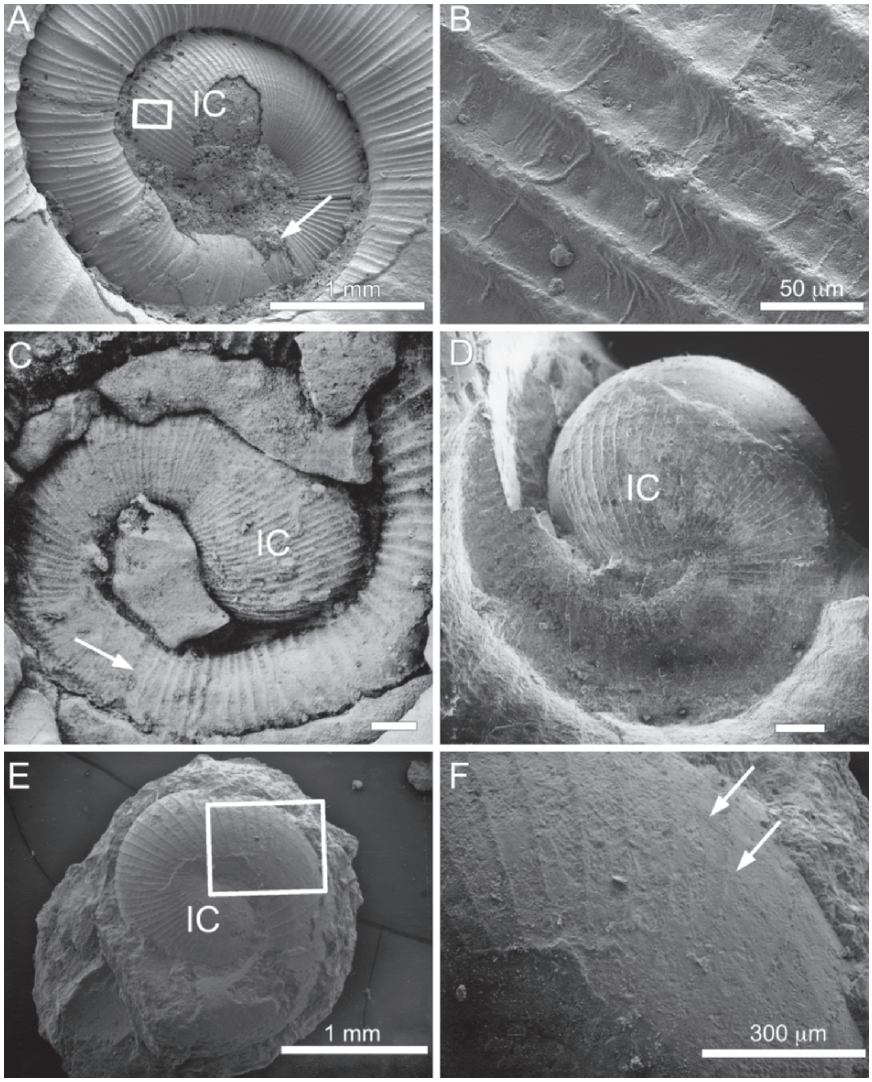


**Fig. 2.1** *Ammonitellas in the families Mimagoniatidae and Agoniatitidae. (A, B)* Archanarcestes obesus *(AMNH 45370, Devonian, Morocco). (A) Lateral view of ammonitella. The initial chamber (IC) is visible and the end of the ammonitella is marked by breakage of the shell (arrow). Scale bar = 1.00 mm. (B) Close-up of transverse lirae on the initial chamber IC showing well-developed lirae with "wrinkle-like" creases stretched perpendicular between them. Area of photograph is marked by a box in 1A. Scale bar = 50.0 µm. (C)* Archanarcestes obesus *(AMNH 45374, Devonian, Morocco). Lateral view of ammonitella showing the initial chamber IC and primary constriction (arrow). Scale bar = 200 µm. (D)* Agoniatites vanuxemi *(NYSM 3545, Devonian, New York State). Lateral view of ammonitella. Scale bar = 200 µm. (E, F)* Fidelites fidelis *(AMNH 50417, Devonian, Morocco). (E) Lateral view of ammonitella showing the flattening on the ventral side of the ammonitella. Scale bar = 1.00 mm. (F) Close-up of transverse lirae showing faint, perpendicular "wrinkle-like" creases (arrows) between them. Area of close-up is indicated by a box on 1E. Scale bar = 300 µm.*

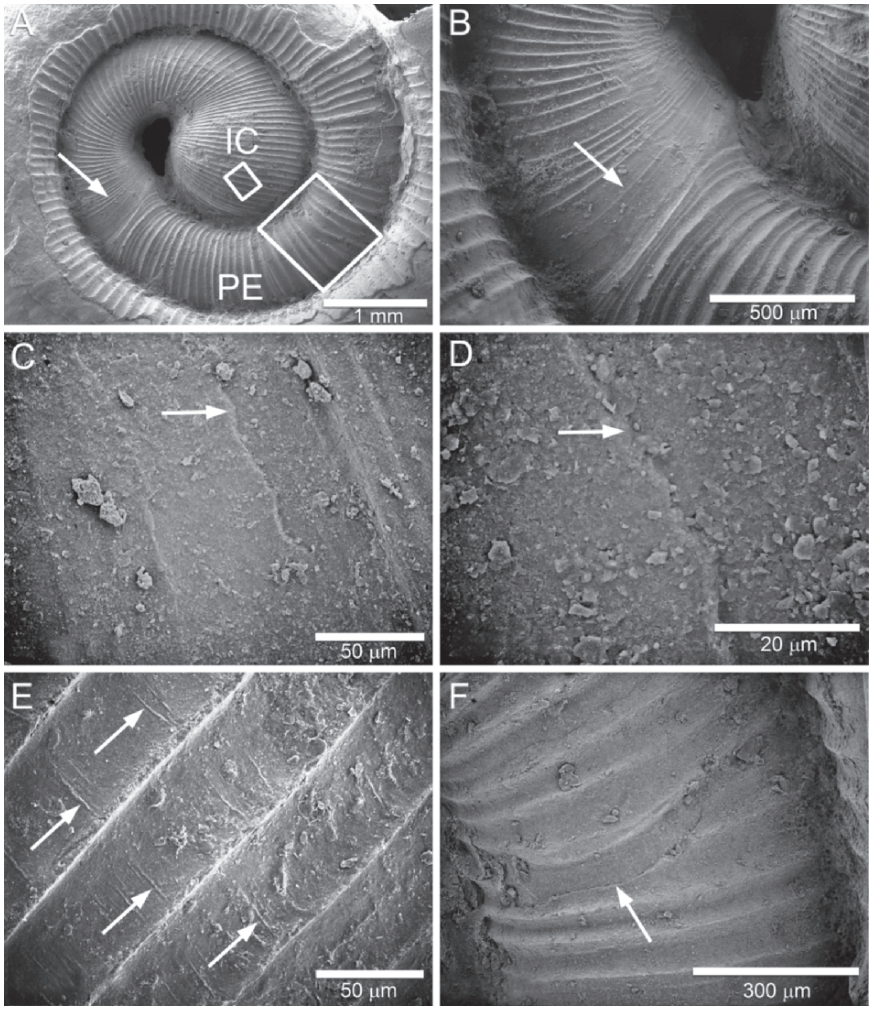


**Fig. 2.2** Mimagoniatites fecundus *(AMNH 46645, Devonian, Morocco). (A) Lateral view of ammonitella showing initial chamber (IC), the apertural edge of ammonitella (arrow), and about one-half whorl of postembryonic shell (PE). Scale bar = 1.00 mm. (B) Close-up of aperture (arrow) showing the reduction in size and spacing of transverse lirae. Postembryonic shell is to the right. Scale bar = 500 μm. (C) Close-up from B, rotated approximately 45° to the right, showing the apertural edge of the ammonitella (arrow). The postembryonic shell can be seen emerging from beneath the ammonitella edge on the right. Scale bar = 50.0 μm. (D) Close-up of the apertural edge of the ammonitella from C (arrow). Scale bar = 20.0 μm. (E) Close-up of the transverse lirae on the initial chamber IC showing the "wrinkle-like" creases stretched perpendicularly between them (arrows). Area of photograph is indicated by the small box on the initial chamber IC in 2A. Scale bar = 50.0 μm. (F) Close-up of the postembryonic shell showing a healed break in the shell (arrow) which disrupted the production of the ornament. Area of close-up is indicated by box on the postembryonic shell in 2A. Scale bar = 300 μm.*

Most studies on ammonitellas are based on well-preserved Mesozoic specimens and it has been inferred that at least some of the same features could be extrapolated to the earliest Devonian forms (Schimansky, 1954; Erben et al., 1968; Kulicki, 1974, 1979; Drushschits et al., 1977; Bandel, 1982; Tanabe, 1989; Landman et al., 1996). The significance of these features and their implication for embryonic development has, however, been debated (see Klofak et al., 1999). Studies on Devonian taxa have demonstrated that many of the features defined for Mesozoic forms are present in their Devonian predecessors, for example, the prosiphon, caecum, and primary constriction (Klofak et al., 1999). There are critical differences, such as the ornament on the shell. In the advanced Paleozoic and Mesozoic ammonoids, the surface of the embryonic shell is either smooth or covered with fine tubercles (Tanabe et al., 1994; Landman et al., 1996; Sprey, 2002). In Devonian taxa the ammonitella is covered by transverse lirae (Clarke, 1899; Miller, 1938; Erben, 1960, 1964b; Clausen, 1969; House, 1996; Klofak et al., 1999). Another important difference occurs at the end of the ammonitella. In post-Devonian ammonoids the primary (or nepionic) constriction is accompanied by a thickening of the shell wall called the primary varix. Studies of well-preserved material have shown that this varix is absent in Devonian ammonoids (Klofak et al., 1999).

These differences have fueled much of the debate as to how the ammonitellas of Devonian ammonoids formed. Most models for post-Devonian ammonitellas call for a nonaccretionary mode of growth because these ammonitellas do not possess any ornament that might be interpreted as having formed by marginal accretion at the aperture. Devonian ammonoids, however, possess transverse lirae, which has suggested to some authors that these embryonic shells formed in an accretionary way (Erben, 1964b, 1966; Erben et al., 1968; Tanabe, 1989). The embryonic lirae are structurally different from those found on the postembryonic shell, however, which might suggest that the embryonic and postembryonic shell formed differently (Klofak et al., 1999). A similar situation has been described for Jurassic ammonites (Kulicki, 1974, 1979; Sprey, 2002) and Triassic ceratites (Landman et al., 2001). The authors in all of these studies describe tuberculate micro-ornament on both the embryonic and postembryonic shell. The morphology of the embryonic and postembryonic tubercles is different in each case, and, hence, it is likely that the two parts of the shell formed differently. Ultimately, the solution may lie in finding and examining shell microstructure, something we have not yet been able to do for Devonian ammonoids.

Previous descriptions of Devonian ammonitellas have been incorporated in numerous taxonomic descriptions (Miller, 1938; Erben, 1953, 1960, 1964b; Petter, 1959; House, 1962; Bogoslovsky, 1969; Chlupáč and Turek, 1983; Bensaïd, 1974; Göddertz, 1987, 1989; Wissner and Norris, 1991; Klug, 2001). Commonly, the size (diameter) and shape of the initial chamber and the degree of coiling of the ammonitella are given. Descriptions of lirae have generally been limited to noting their presence, largely due to the lack of well-preserved material. The exception is Erben (1964b) who described the pattern of the lirae in several Devonian taxa.

Our study entails an examination and quantification of the lirae of well-preserved ammonitellas from three families of Devonian ammonoids: the Mimagoniatitidae,

the Anarcestidae, and the Agoniatitidae. The three families are all closely related phylogenetically, albeit of different taxonomic rank. Most workers have placed them within the same higher taxonomic group whether it be the superfamily Agoniatitacea (Miller, 1938), superfamily Anarcestaceae (Miller and Furnish, 1954; Petter, 1959; Erben, 1964b), suborder Agoniatitina (Bogoslovsky, 1969; House, 1981), order Anarcestida (Becker and House, 1994), or order Agoniatitida (Ruzhentsev, 1960, 1974; Becker and Kullmann, 1996; Korn, 2001; Korn and Klug, 2002). In most previously proposed phylogenies, the Mimagoniatitidae are viewed as ancestral to both the Agoniatitidae and the Anarcestidae, but generally more closely related to the Agoniatitidae. For example, within his superfamily Agoniatitacea, Miller (1938) placed the Mimagoniatitinae and Agoniatitinae in the family Agoniatitidae and the Anarcestinae in their own family, the Anarcestidae. More recently, the mimagoniatids and agoniatids were placed within the suborder Agoniatitina and the anarcestids were placed within the Anarcestina, both within the order Agoniatitida (Becker and Kullmann, 1996; Korn, 2001).

It is hoped that a study of the pattern of lirae spacing on the ammonitella may reveal data useful in defining both how the individual lirae as well as the ammonitella as a whole formed. By including data from three related families, the pattern of lirae spacing can then be compared among taxa. Differences that emerge may define useful taxonomic characters. They may also aid in our understanding of the early radiation of the Ammonoidea.

## 2 Material and Methods

The taxa used in this study are: *Archanarcestes obesus* (Erben, 1960) and *Mimagoniatites fecundus* Barrande, 1865, from the Mimagoniatitidae; *Agoniatites vanuxemi* (Hall, 1879) and *Fidelites fidelis* Barrande, 1865, from the Agoniatitidae; and *Latanarcestes* sp. from the Anarcestidae. Six of the specimens are from Morocco. The remaining specimen (*A. vanuxemi*) is from the Cherry Valley Limestone of New York State (see Clarke, 1899). Descriptions of Moroccan localities are given below. For a more detailed description of the geology and stratigraphy of these localities, see Becker and House (1994) and Klug (2000).

AMNH locality 3233: *Archanarcestes obesus* (AMNH 43374) from layer "4B" (Becker and House, 1994). Lower-Middle Devonian. East of Bou Tcharfine, near Erfoud, Morocco; latitude 31° 16′ 46″ N, longitude 3° 53′ 0.54″ W.

AMNH locality 3237: *Archanarcestes obesus* (AMNH 45370), Emsian, Devonian. Bou Tcharfine, near Erfoud, Morocco.

AMNH locality 3311: *Mimagoniatites fecundus* (AMNH 46645) and *Latanarcestes* sp. (AMNH 46646 and 50416). Emsian, Devonian. East of Bou Tcharfine, near Erfoud, Morocco; latitude 31° 22.51′ N, longitude 4° 4.38′ W.

AMNH locality 3312: *Fidelites fidelis* (AMNH 50417). Late Emsian, Devonian. Jebel Ouaoufilal, near Taouz, Tafilalt; latitude 30° 55.93′ N, longitude 4° 1.14′ W.

Specimens were examined using the scanning electron microscope (SEM). Four of these specimens have been previously illustrated (Klofak et al., 1999); three specimens are studied for the first time. AMNH 45374 described in Klofak et al. (1999) is revised here as *Archanarcestes obesus*.

Ornament was examined to confirm previous findings and expand the database. In addition to qualitative observations, measurements were collected on the distance between lirae on both the ammonitella and postembryonic shell. Measurements were taken from SEM photographs using the Quartz PCI Imaging Management System. Measurements were taken from three positions on the shell, wherever possible: ventral, midflank, and dorsal (Fig. 2.5a). The ventral and dorsal measurements were not taken directly on the venter or dorsum, but as close as possible in lateral view. The midflank measurements were taken along a line on the middle part of the flank. This represents the point of maximum whorl width. Measurements began at the apex of the shell and extended to the aperture of the embryonic shell. "Distance 1" is the distance between the first and second lirae measured between the crests of successive lirae (Fig. 2.5b); "distance 2" is the distance between the crests of the second and third lirae, and so forth. Measurements began at the closest measurable lira starting at the apex. Postembryonic lirae are designated in the same manner with the first postembryonic lirae distance designated "distance 1."

Specimens used in this study are reposited in the American Museum of Natural History, New York, New York (AMNH), and the New York State Museum, Albany, New York (NYSM).

# 3 Results

## 3.1 External Features of the Ammonitella

Ornament for all taxa consists of transverse lirae that cover the entire ammonitella except for a "bald spot" at the apex (Klofak et al., 1999). "Wrinkle-like" creases stretch between the lirae and are best defined on the initial chamber. These "wrinkle-like" creases are most strongly expressed in the Mimagoniatitidae (Figs. 2.1b, 2.2e), less strongly expressed in the Anarcestidae (Fig. 2.3b), and least strongly expressed in the Agoniatitidae (Fig. 2.1f).

The lirae are a relief feature and are not preserved on the steinkern as shown in *Latanarcestes* where the shell is broken away on part of the initial chamber (Fig. 2.3a, c, d; see also Klofak et al., 1999: Figs. 3c, 8b). The lirae on the embryonic shell differ from those on the postembryonic shell in that the embryonic lirae are symmetrical, while the postembryonic lirae are asymmetrical and more steeply sloped on the apical side (Klofak et al., 1999).

Just adapical of the primary constriction, the lirae become much weaker and more closely spaced (Figs. 2.2b, 2.3d, 2.4b). The edge of the ammonitella is marked by a primary constriction, with no evidence of an accompanying varix in any speci-

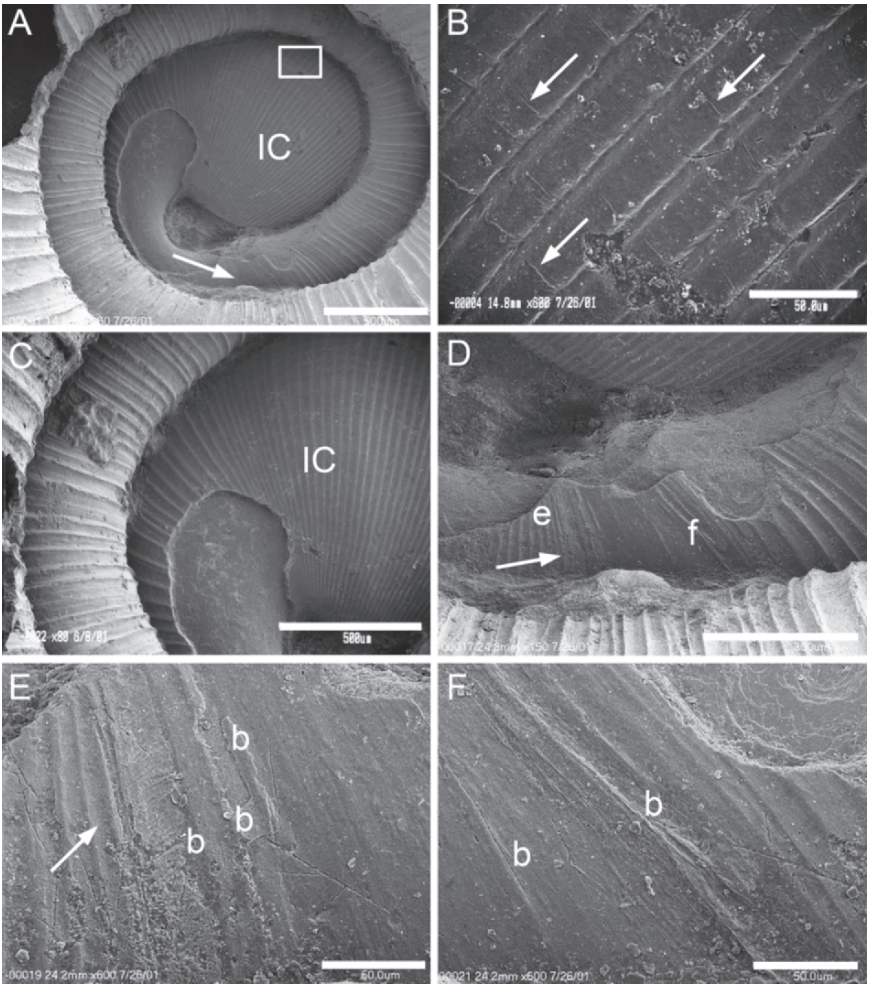


**Fig. 2.3** Latanarcestes *sp. (AMNH 46646, Devonian, Morocco). (A) Lateral view of ammonitella showing initial chamber (IC) and part of apertural edge of ammonitella (arrow). Scale bar = 1.00 mm. (B) Close-up of transverse lirae on initial chamber IC showing perpendicular "wrinkle-like" creases (arrows) stretched between them. Area of close-up is indicated by a box on 3A. Scale bar = 50.0 μm. (C) Close-up near the end of the initial chamber IC where shell has broken away exposing the steinkern. Note that the surface of the steinkern is smooth, unaffected by the ornament on the shell. Scale bar = 500 μm. (D) Close-up of ammonitella showing the apertural edge of the ammonitella (arrow). Scale bar = 80.0 μm. (E) Close-up of the apertural edge of the ammonitella (arrow) showing the postembryonic shell emerging from beneath it and followed by a series of breaks (b) in the postembryonic shell, with new shell emerging from beneath the existing shell. Area of close-up marked by letter e in 3D. Scale bar = 50.0 μm. (F) Close-up of smooth area of postembryonic shell to the right of 3E showing a series of breaks (b) with new shell emerging from beneath the existing shell. Area of close-up is marked by letter f in 3D. Scale bar = 50.0 μm.*

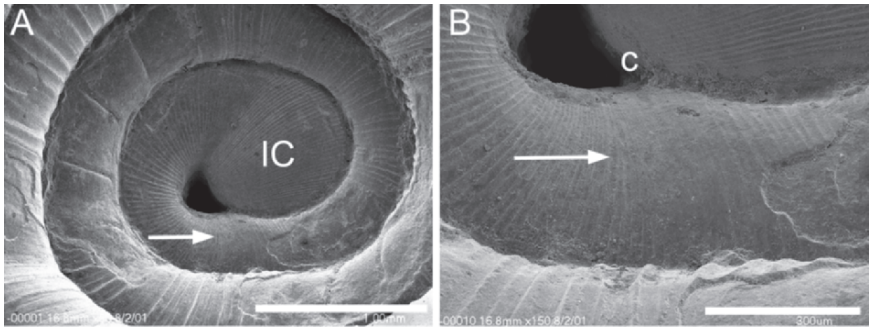


**Fig. 2.4** Latanarcestes *sp. (AMNH 50416, Devonian, Morocco). (A) Lateral view of ammonitella showing initial chamber (IC), with visible constriction (arrow). Scale bar = 1.00 mm. (B) Close-up of apertural edge of ammonitella (arrow). Constriction is visible on dorsal edge (c). Scale bar = 300 μm.*

men examined (Figs. 2.2b, c, d, 2.3d, e, f, 2.4b). In previously studied specimens, the apertural edge of the ammonitella appears as a crease or break (Fig. 2.1a, c; see also Klofak et al., 1999). A perfectly preserved aperture is present in a specimen of *Archanarcestes obesus* (Fig. 2.2b, c, d) where the apertural edge parallels the ornament and forms a distinct line across the flank, slightly irregular in appearance. The postembryonic shell can be seen emerging from beneath the embryonic shell (Fig. 2.2c, d). This occurs in the area of smaller, finer lirae. In *Latanarcestes* sp., the area of small faint lirae is more extensive when compared to the specimens of *Archanarcestes* (Figs. 2.3d, 2.4b; see also Klofak et al., 1999: Fig. 8d). The apertural edge also appears in this area and, like *Archanarcestes,* is irregular in its course. Multiple breaks occur adoral of the apertural edge with successive shell layers emerging from beneath the previously secreted shell (Fig. 2.3e, f).

## 3.2 Lirae Spacing

The second part of our study is an analysis of lirae spacing in three of the earliest families of ammonoids: the Mimagoniatitidae, the Anarcestidae, and the Agoniatitidae. In total, seven specimens were studied; three mimagoniatids, two anarcestids, and two agoniatids.

The results are presented in Figs. 2.6–2.11. The horizontal axis is the lirae number beginning with the most adapical lira on the embryonic shell; in some graphs, the first lira measured is on the postembryonic shell. The vertical axis is the distance between lirae (see Fig. 2.5b), given in microns. Data are presented for the three measured positions: ventral, midflank, and dorsal (Fig. 2.5a). They are graphed together using different symbols for each position on the shell. Data are given in Appendices 1–11.

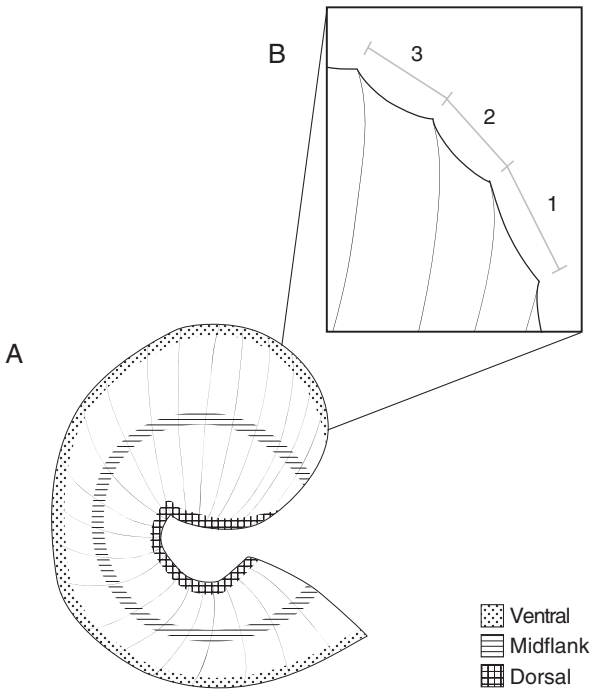


**Fig. 2.5** *Sketch of the ammonitella of a primitive ammonoid showing the areas where the lirae spaces (distances between successive lirae) were measured. (A) The three areas are marked with different patterns: Ventral = dots; Midflank = horizontal lines; and Dorsal = cross hatch. (B) Close-up of ventral edge of ammonitella with lirae shown raised. The horizontal line (1, 2, 3) indicates how the distances were measured.*

The ratios of the ventral (V) and dorsal (D) lirae distance are also given, where possible. The horizontal axis is the lirae number and the vertical axis is the ratio (V/D).

Means and standard deviations were calculated for the distance between lirae using data from the midflank position. Data are given in Table 2.1. Because of the extent of the overlap of standard deviations, these data cannot be used to differentiate among the three taxonomic groups. The results of an F-test confirm that the means are significantly different at the 0.01 level.

### 3.2.1 Mimagoniatitidae

The three specimens from the Mimagoniatitidae show the same general pattern, although there is some variation (Figs. 2.6a, 2.7a, 2.8a). Two of the specimens are *Archanarcestes obesus* (AMNH 45374, Fig. 2.7, Appendix 2; AMNH 45370, Fig. 2.8, Appendix 1).

**Table 2.1** *Means of the distance between successive lirae calculated at the mid flank positions. Measurements are given in microns.*

| | | Lirae spacing (μm) | |
|---|---|---|---|
| Family | N | Mean ± SD | Range |
| MIMAGONIATIDAE | | | |
| AMNH 46645 | 76 | 45 ± 16 | 14–75 |
| AMNH 45374 | 52 | 31 ± 9 | 9–49 |
| AMNH 45370 | 55 | 28 ± 10 | 14–52 |
| AGONIATITIDAE | | | |
| NYSM 3545 | 56 | 40 ± 8 | 55–25 |
| AMNH 50417 | 29 | 47 ± 15 | 28–126 |
| ANARCESTIDAE | | | |
| AMNH 46646 | 70 | 28 ± 10 | 8–70 |
| AMNH 50416 | 94 | 18 ± 6 | 10–37 |

The third specimen is *Mimagoniatites fecundus* (AMNH 46645, Fig. 2.6, Appendix 4). As expected, based on simple geometry, the ventral distance between lirae is greater than the dorsal distance because the venter subscribes a greater arc. The midflank position contains measurements midway between the dorsum and venter.

There is a general increase in the distance between lirae over the initial chamber at the ventral, midflank, and dorsal positions. Then at approximately 5–10 lirae from the apex, there is a decrease in the distance. This is generally slight, but in one specimen (AMNH 45374, Fig. 2.7a), it is expressed very strongly. After this initial drop, there is a second increase, followed by an abrupt drop in lirae distance in all three specimens. This decrease marks the end of the initial chamber and occurs at about 25–30 lirae from the apex. Over the course of the ammonitella coil, there is a gentle increase in spacing followed by a decrease at the ventral, midflank, and dorsal positions. This decrease is abrupt and occurs at the end of the ammonitella. In all, there are 70–77 lirae on the ammonitella of the Mimagoniatitidae.

The spacing between lirae can fluctuate within the general trend. There appears to be no pattern to this fluctuation. The result is a graph with a very jagged appearance. These fluctuations are also not perfectly aligned among the three measured positions.

In two of the specimens (AMNH 46645, Fig. 2.6b, Appendix 5; AMNH 45374, Fig. 2.7b, Appendix 3), the postembryonic distance between lirae was measured. Again, the ventral distance was the widest, the dorsal distance was the narrowest, and the midflank distance was in between. There is a rapid increase in spacing from the first measurable postembryonic lira.

The ratio of the ventral distance/dorsal distance (V/D) on the embryonic shell was compared to that of the postembryonic shell (Figs. 2.6c, d, 2.7c, d). The most complete data set (AMNH 46645) shows that there is much greater correlation between the dorsal and ventral distances between lirae on the postembryonic shell than on the embryonic shell (Fig. 2.6c, d).

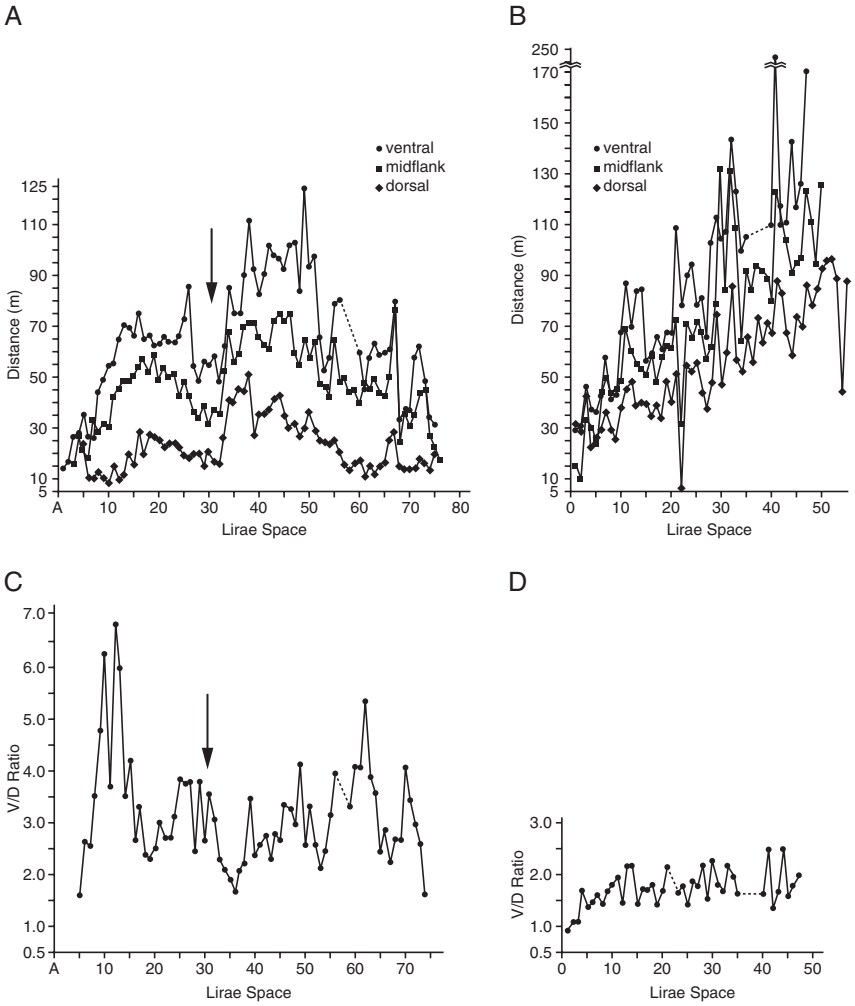


**Fig. 2.6** Mimagoniatites fecundus *(AMNH 46645, Devonian, Morocco). (A) Lirae spacing on embryonic shell for ventral, midflank, and dorsal positions. Symbols given in graph. The X axis is the number of lirae space (see methods and materials for details). The Y axis is the measured distance between two lirae given in microns (μm). Data are given in Appendix 4. (B) Lirae spacing on postembryonic shell for ventral, midflank, and dorsal positions. The X axis is the number of lirae space. The Y axis is the measured distance between two lirae given in microns (μm). Data are given in Appendix 5. (C) Ratio of the ventral lirae space/dorsal lirae space (V/D) on the embryonic shell. Data are given in Appendix 4. (D) Ratio of the ventral lirae space/dorsal lirae space (V/D) on the postembryonic shell. Data are given in Appendix 5.*

### 3.2.2 Anarcestidae

Two specimens from the Anarcestidae were measured, both identified as *Latanarcestes* sp. (AMNH 46646 and AMNH 50416). The results are presented in

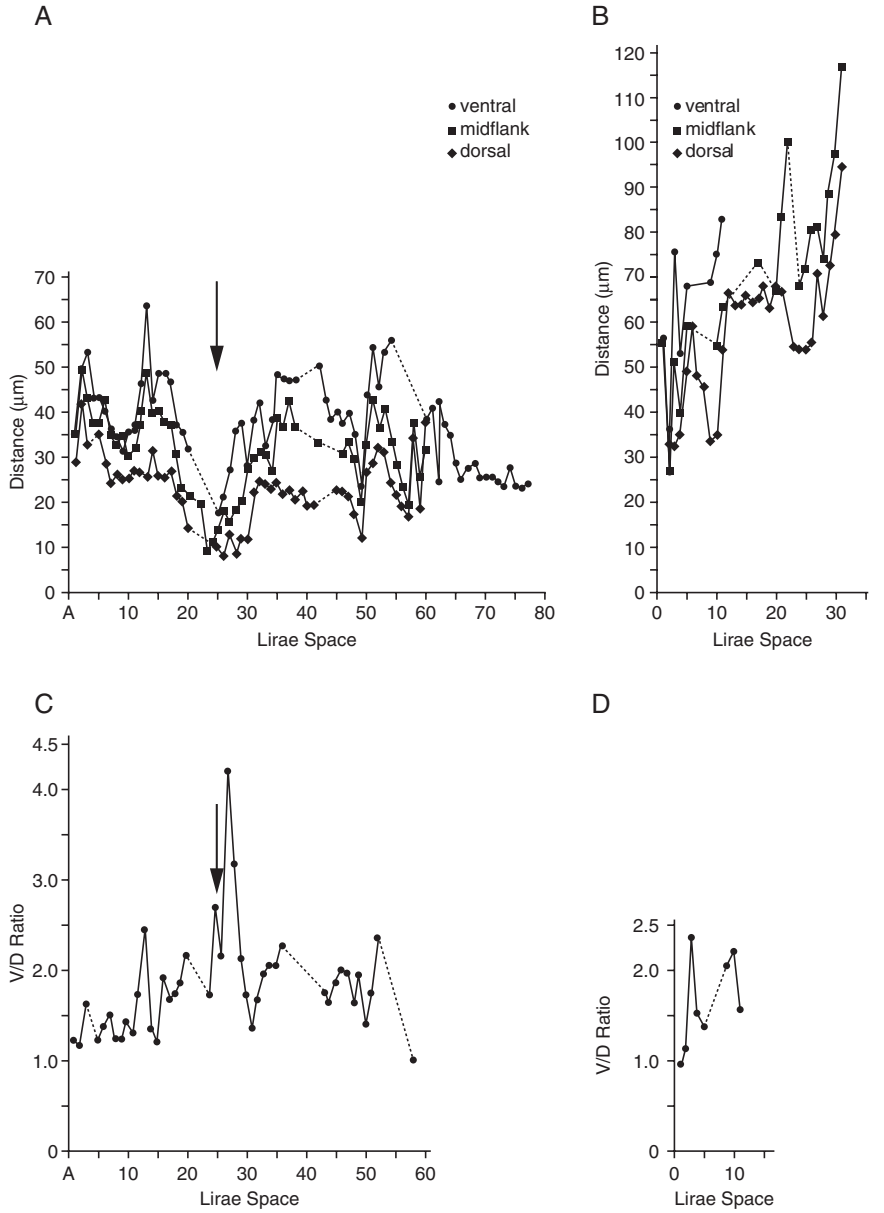


**Fig. 2.7** Archanarcestes obesus *(AMNH 45374, Devonian, Morocco). (A) Lirae spacing on embryonic shell for ventral, midflank, and dorsal positions. Symbols given in graph. X axis is the number of lirae space. Y axis is the measured distance between two lirae given in microns (µm). Data are given in Appendix 2. (B) Lirae spacing on postembryonic shell for ventral, midflank, and dorsal positions. X axis is the number of lirae space. Y axis is the measured distance between two lirae given in microns (µm). Data are given in Appendix 3. (C) Ratio of the ventral lirae space/dorsal lirae space (V/D) on the embryonic shell. Data are given in Appendix 2. (D) Ratio of the ventral lirae space/dorsal lirae space (V/D) on the postembryonic shell. Data are given in Appendix 3.*

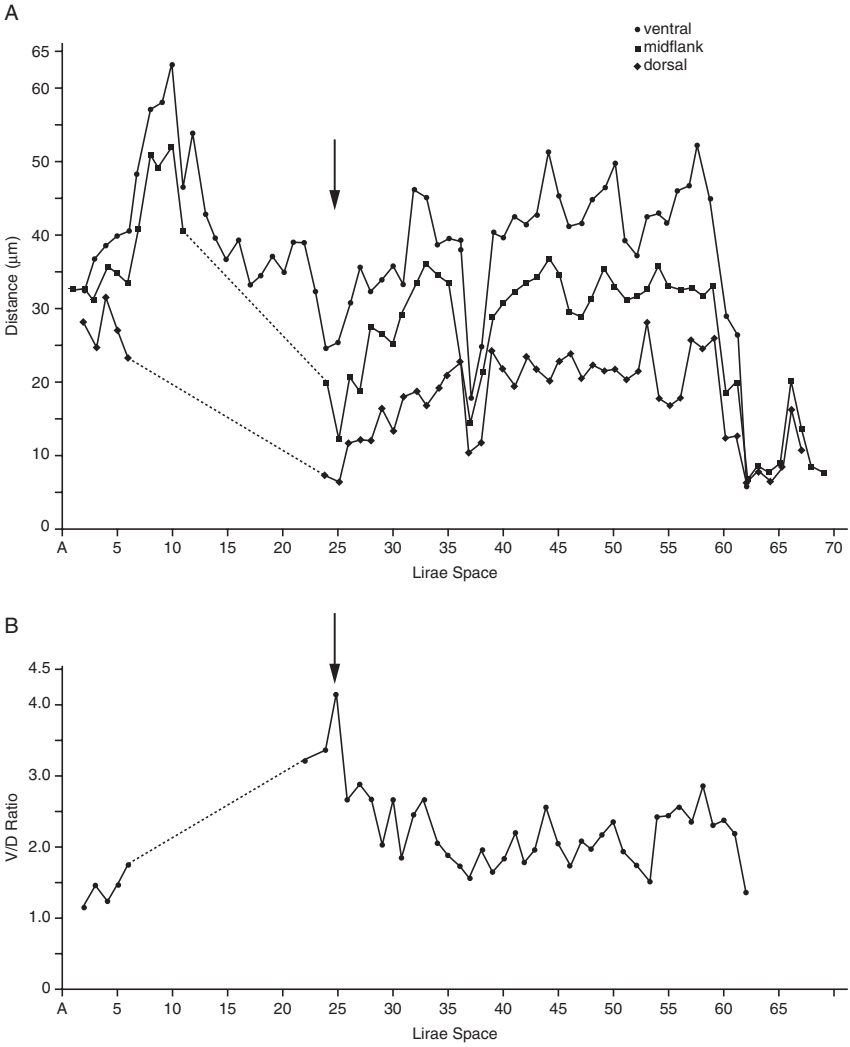


**Fig. 2.8** Archanarcestes obesus *(AMNH 45370, Devonian, Morocco). (A) Lirae spacing on embryonic shell for ventral, midflank, and dorsal positions. Symbols given in graph. X axis is the number of lirae space. Y axis is the measured distance between two lirae given in microns (µm). (B) Ratio of the ventral lirae space/dorsal lirae space (V/D) on the embryonic shell. Data are given in Appendix 1.*

Figs. 2.9–2.10 and Appendices 6–9. Except for a small gap, the data for AMNH 50416 are complete across the ammonitella (Fig. 2.9a). AMNH 46646 has dorsal measurements for only the initial chamber (Fig. 2.10a). Thereafter, the ventral data are the most complete. On the initial chamber, as in the Mimagoniatitidae, the ventral distance is the widest, the dorsal the narrowest, and the midflank somewhere in between. The ventral distance increases, then decreases to the end of the initial

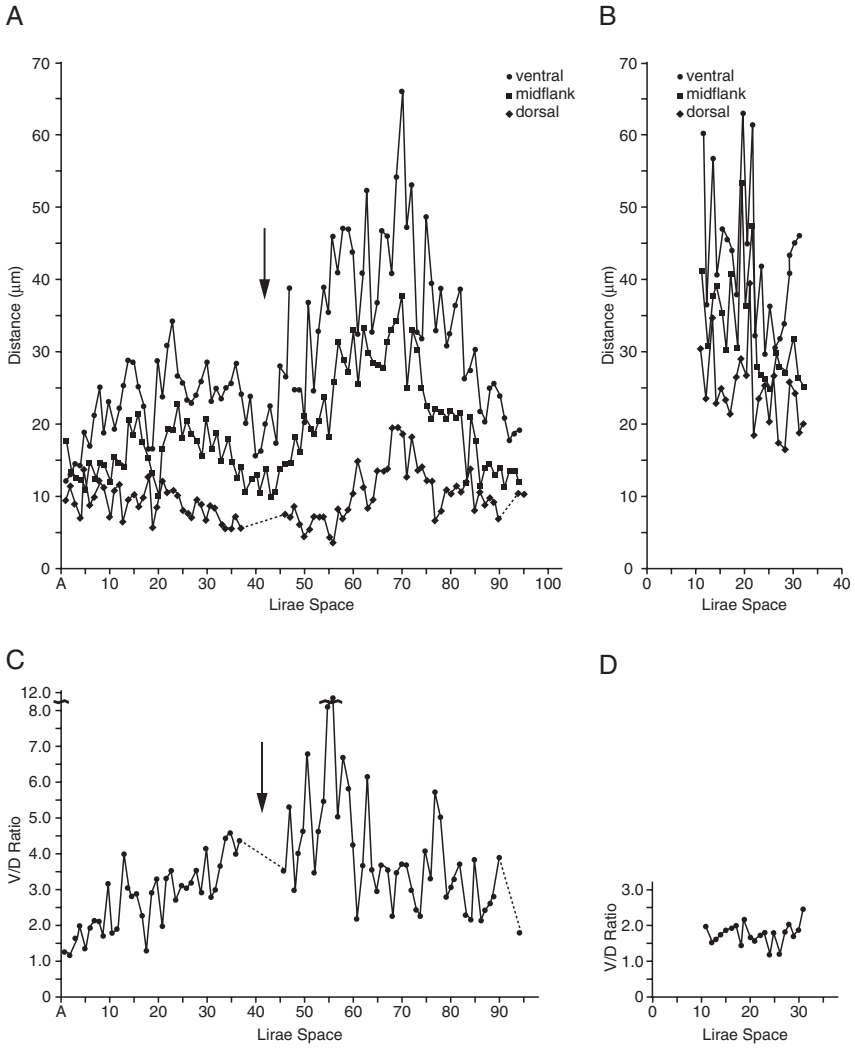


**Fig. 2.9** Latanarcestes *sp. (AMNH 50416, Devonian, Morocco). (A) Lirae spacing on embryonic shell for ventral, midflank, and dorsal positions. Symbols given in graph. X axis is the number of lirae space. Y axis is the measured distance between two lirae given in microns (µm). Data are given in Appendix 8. (B) Lirae spacing on postembryonic shell for ventral, midflank, and dorsal positions. X axis is the number of lirae space. Y axis is the measured distance between two lirae given in microns (µm). Data are given in Appendix 9. (C) Ratio of the ventral lirae space/dorsal lirae space (V/D) on the embryonic shell. Data are given in Appendix 8. (D) Ratio of the ventral lirae space/dorsal lirae space (V/D) on the postembryonic shell. Data are given in Appendix 9.*

chamber, seen most strongly in AMNH 50416 (Fig. 2.9a). The pattern of midflank distance parallels that of the ventral distance. The dorsal distance, in contrast, decreases slowly from the apical end of the initial chamber to its end. A decrease in the distance between lirae marks the end of the initial chamber in the ventral and midflank data. There are 40–45 lirae on the initial chamber.

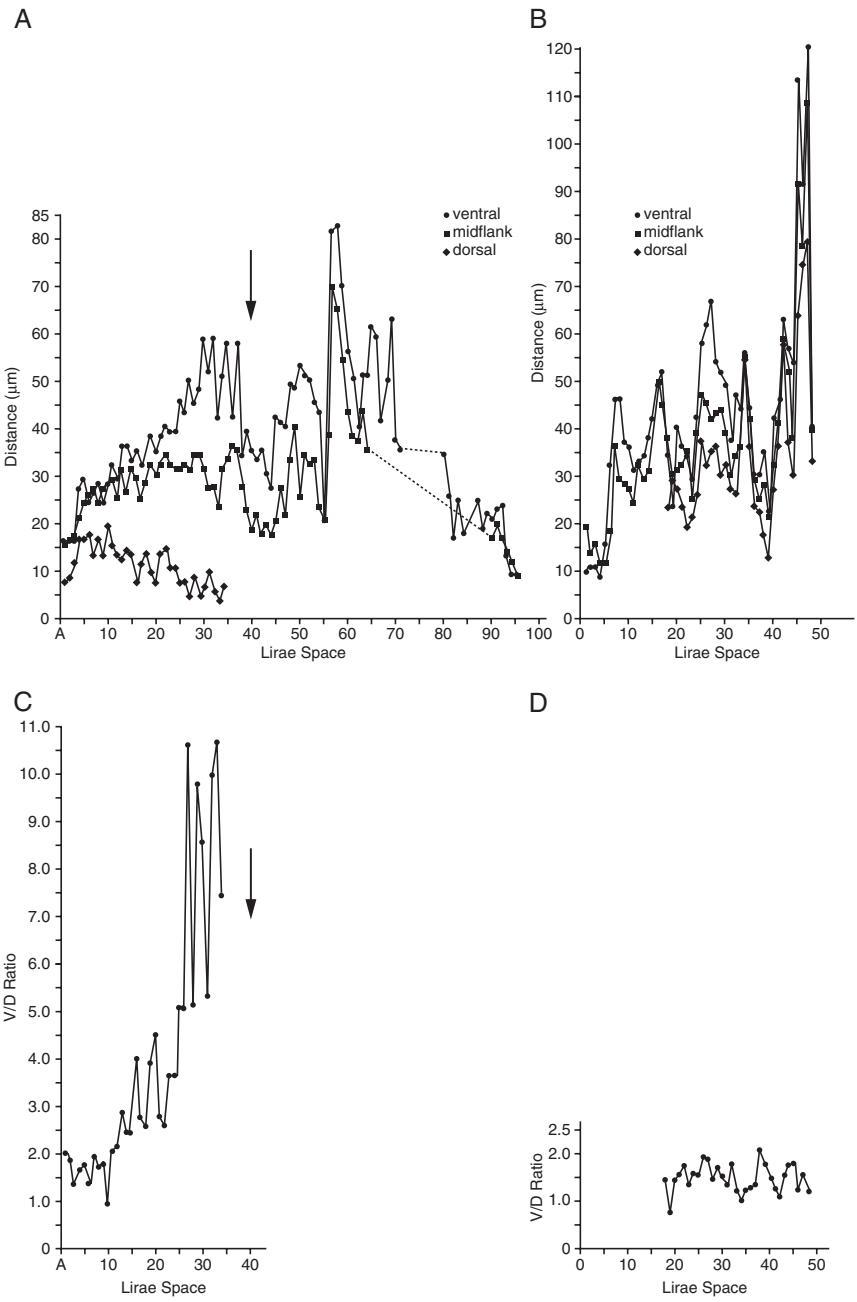


**Fig. 2.10** Latanarcestes *sp. (AMNH 46646, Devonian, Morocco). (A) Lirae spacing on embryonic shell for ventral, midflank, and dorsal positions. Symbols given in graph. X axis is the number of lirae space. Y axis is the measured distance between two lirae given in microns (µm). Data are given in Appendix 6. (B) Lirae spacing on postembryonic shell for ventral, midflank, and dorsal positions. X axis is the number of lirae space. Y axis is the measured distance between two lirae given in microns (µm). Data are given in Appendix 7. (C) Ratio of the ventral lirae space/dorsal lirae space (V/D) on the embryonic shell. Data are given in Appendix 6. (D) Ratio of the ventral lirae space/dorsal lirae space (V/D) on the postembryonic shell. Data are given in Appendix 7.*

Immediately after the decrease in distance, there is an increase in distance on the ammonitella coil. This peaks at about 20 lirae from the end of the initial chamber. Adoral of this, the distance decreases on the ammonitella coil until the end of the ammonitella. This pattern is observed on the dorsal, midflank, and ventral positions (Figs. 2.9a, 2.10a). There are 95 lirae on the ammonitella of these Anarcestidae. The distances of the postembryonic lirae show no initial increase, just wide fluctuations (Figs. 2.9b, 2.10b). Only after about 40 lirae does the distance between the lirae begin to increase.

The V/D ratios again show a greater amount of fluctuation between successive lirae on the embryonic shell when compared to the postembryonic shell (Figs. 2.9c, d, 2.10c, d).

### 3.2.3 Agoniatitidae

Two specimens from the Agoniatitidae were studied, identified as *Agoniatites vanuxemi* (NYSM 3545) and *Fidelites fidelis* (AMNH 50417). The data are presented on Fig. 2.11 and Appendices 10–11. It was not possible to measure the distance between lirae on the postembryonic shell. The data for the two Agoniatitidae are less complete than those for the Mimagoniatitidae and the Anarcestidae. There are gaps in various places at all three measurement positions. In *F. fidelis*, the lirae can only be measured to just adoral of the initial chamber (Fig. 2.11b). Here again, the ventral distance is the widest, the dorsal the narrowest, and the midflank measurement lies somewhere in between. In both genera, after an initial increase in the distance between lirae (1–10) at all three positions, there is a slight decrease. Then, at the ventral and midflank positions, the distance increases rapidly to the end of the initial chamber. At the dorsal position, however, the distances vary widely, but remain essentially level. There are about 30–35 lirae on the initial chamber. There is a decrease at the end of the initial chamber, followed by a very rapid increase in the distance between lirae at the ventral and midflank position and a less rapid increase at the dorsal position. For the remainder of the ammonitella in *A. vanuxemi* (Fig. 2.11a), there is a rapid decrease in the distance followed by a more gradual increase, then a leveling off or a slight decrease. Data end just before the end of the ammonitella in both specimens. There are approximately 65 lirae on the ammonitella of the Agoniatitdae.

Because of gaps in the data, there are fewer data available for calculation of the V/D ratio. What is evident is that over the initial chamber, the ratio increases rapidly at about 20 lirae (V > > D) and reaches a maximum at this point (Fig. 2.11c, d).

## 4 Discussion

These specimens confirm previous findings on the nature of the ammonitella of early Devonian ammonoids (Klofak et al., 1999). The end of the ammonitella is marked by a reduction in both the spacing and size of the ornament, until a relatively smooth surface appears. A constriction is present with no accompanying

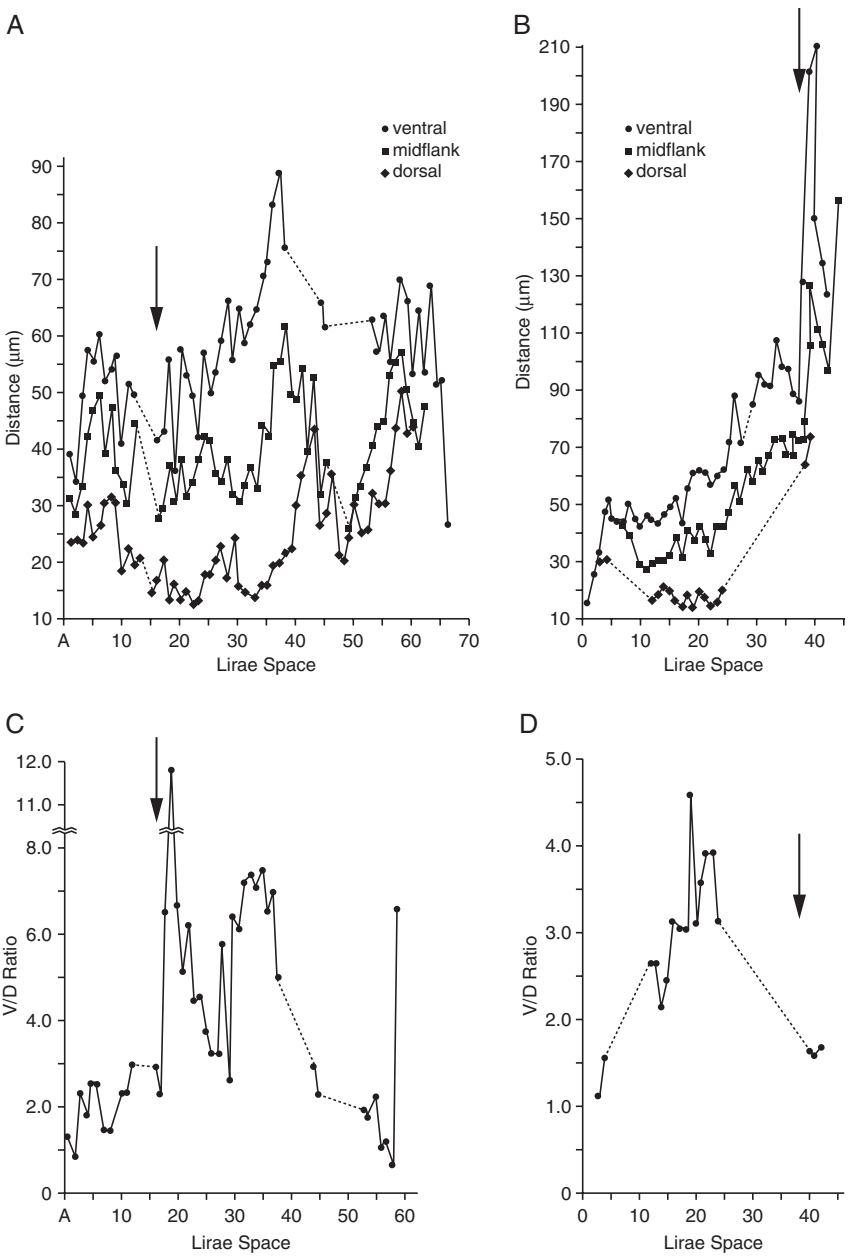


**Fig. 2.11** *(A, C)* Agoniatites vanuxemi *(NYSM 3545, Devonian, New York State, USA) (A) Lirae spacing on embryonic shell for ventral, midflank, and dorsal positions. Symbols given in graph. X axis is the number of lirae space. Y axis is the measured distance between two lirae given in microns (µm). (C) Ratio of the ventral lirae space/dorsal lirae space (V/D) on the embryonic shell. Data are given in Appendix 10. (B, D)* Fidelites fidelis *(AMNH 50417, Devonian, Morocco). (B) Lirae spacing on embryonic shell for ventral, midflank, and dorsal positions. Symbols given in graph. X axis is the number of lirae space. Y axis is the measured distance between two lirae given in microns (µm). (D) Ratio of the ventral lirae space/dorsal lirae space (V/D) on the embryonic shell. Data are given in Appendix 11.*

varix. Previously, the absence of a primary varix was documented for the genus *Archanarcestes* in the family Mimagoniatitidae (see Klofak et al., 1999). A second genus in the Mimagoniatitidae demonstrates the same type of ammonitella aperture, that is, a constriction with no varix. Finally, we have also extended this apertural type to a second family, the Anarcestidae. It is known that a varix is present in the Tornoceratina (House, 1965), a phylogenetically more advanced taxon (Becker and Kullmann, 1996; Klug and Korn, 2002). To date, no varix has been found in phylogenetically more primitive ammonoids, increasing the likelihood that this may be the ancestral state for ammonoids. Bactritids also do not possess a varix, but the microstructure of their embryonic shells is different from that of these ammonitellas and may represent a different mode of formation. Bactritids are different enough that some workers have separated them from the Ammonoidea (Ruzhentshev, 1960, 1974; Erben, 1964a; Mapes, 1979; Doguzhaeva, 2002; Korn and Klug, 2002).

The postembryonic shell can be seen emerging from beneath the ammonitella edge of several specimens (AMNH 46646, Fig. 2.3f; AMNH 46645, Fig. 2.2c, d). In the specimen of *Latanarcestes,* the area just anterior to the ammonitella edge shows several breaks, with new shell emerging from below the previous surface (Fig. 2.3f). This is not dissimilar to the end of the embryonic shell in modern *Nautilus* where the thin apertural edge is prone to breakage at hatching (Arnold et al., 1987). It also supports an idea proposed by Kulicki (1974) that the primary varix in post-Devonian ammonoids evolved to prevent breakage during hatching.

It is also clear from the data collected, that while marking the end of a phase in embryonic development, the end of the initial chamber does not exhibit any discernable breaks in shell production (Fig. 2.3c). There is an obvious change in the shape of the shell (see "1. Wachstums-Änderung" of Erben, 1962, 1964b) and a reduction in the distance between lirae in all three taxa at the end of the intial chamber. In addition, Erben (1964b) noted that the ventral sinus appears at this point, perhaps marking the first appearance of the hyponome. This was part of his reason for interpreting this point as the end of embryonic development, though this interpretation has been disproved. Studies on *Nautilus* have shown that a functional hyponome is present early in embryonic development and its appearance is not correlated with hatching (Tanabe et al., 1991).

The original intent of this project was to discover if there were taxonomic differences in the distance between lirae in different taxonomic groups. It became apparent that there was enough variation across an individual ammonitella that any individual measurement or a mean measurement was not informative (Table 2.1). However, the pattern itself proved to be useful.

Based on the shell geometry of a coiled tube with radial ornament, one would expect the distance between any two lirae to be widest on the venter, narrowest on the dorsum, and somewhere in between on the midflank. Projecting a three dimensional object onto two dimensions may distort some measurements. However, the venter and dorsum are not affected because they are measured in the same plane. Distortion could affect the midflank position on the initial chamber but this is minimized because the midflank measurements always lie between the venter and dorsum. Therefore, the patterns in our data are real and not artifacts of the methodology.

There are differences in the distances between lirae on the initial chamber among the different ammonoid families. In the Mimagoniatitidae, the ventral and dorsal parts of the ammonitella show the same pattern (Figs. 2.6a, 2.7a, 2.8a). This is not the case for the Anarcestidae where, as the ventral distance between lirae increases across the initial chamber, the dorsal distance between lirae decreases (Figs. 2.9a, 2.10a). This is also true for the Agoniatitidae (Figs. 2.11a, b). The distance between lirae on the initial chamber of the Agoniatitidae also shows a rapid increase before the decrease marking the end of the initial chamber. These changes reflect subtle changes in the shape and symmetry of the nearly spherical initial chamber. In the Mimagoniatitidae, the arc of both the dorsum and venter are symmetrical, whereas in the Anarcestidae, the arc of the venter is circular but the dorsum is flattened.

With these data, it might be possible to use the change in the distance between lirae as an indicator of the end of the initial chamber. Currently, the initial chamber is defined based on the appearance of the first septum (proseptum) (Owen, 1878; Branco, 1879–1880; Hyatt, 1883; Schindewolf, 1933; Erben, 1960; Bandel, 1982; Landman et al., 1996). It makes better biological sense to define a developmental stage based on characters that formed or are present at that stage (change in distance between lirae) rather than ones added at a later stage (first septum). In other words, the end of the initial chamber would be the point where the distance between lirae shows a marked decrease.

The actual distance between lirae seems to vary widely across the ammonitella. The only constraint on lirae formation on the ammonitella is that the prescribed number of lirae is present by the end of embryonic development. This number is distinctive and taxonomically significant at a family level: 70–77 are present in the Mimagoniatitidae, 95 in the Anarcestidae, and an estimated 65 for the Agoniatitidae. In the Mimagoniatitidae and the Anarcestidae, the difference in number can be directly attributed to the different number of lirae formed on the initial chamber. There are 25–30 in the Mimagoniatitidae and 35–40 in the Anarcestidae, but approximately the same number occur on the ammonitella coil. For the Agoniatitidae, there seems to be a reduction in the number of lirae on the ammonitella coil. There are 30–35 lirae on the initial chamber, more than that in the Mimagoniatitidae, but only a total of 65 for the ammonitella, less than that in the Mimagoniatitidae. Both the Mimagoniatitidae and Anarcestidae have umbilical perforations; the Agoniatitidae do not. It is likely that the tighter coil of the agoniatitid ammonitellas led to a reduction in the size of the ammonitella coil and, hence, a reduction in the number of lirae. The initial chamber, however, remains large. Not only are the agoniatid ammonitellas more tightly coiled, but also the nature of the coiling appears different. The end of the initial chamber can only be defined based on the fold of the dorsal part of the initial chamber against the dorsal part of the ammonitella coil. The venter shows only a slight flattening, similar to the description given for some ammonitellas of Mesozoic ammonoids (Bandel, 1986; Landman et al., 1996). This is visible in the specimen of *Fidelites fidelis* (Fig. 2.1e).

A comparison of the V/D ratio of the embryonic shell and the beginning of the postembryonic shell in the Mimagoniatitidae and Anarcestidae shows the relationship

between the dorsal and ventral parts of the shell. The V/D ratios for the postembryonic shells show that there is a closer correlation between the placement of the lirae on the dorsal and ventral sides of the postembryonic shell, than in the embryonic stage. This pattern is especially clear in Fig. 2.6c, d.

It is assumed that the embryo inside the egg case would have produced a shell in a constant environment. Upon hatching, the growth of the animal and production of shell would have been affected by many variables in the environment, such as temperature, salinity, food supply, predators, and water currents. For example, in Fig. 2.2f, less than a whorl after hatching, a small repaired break can be observed on the shell. Rather than be constrained by a more constant environment, the variability of the embryonic shell formation speaks of a high degree of developmental plasticity. This variability has already been documented by Erben (1950) where he observed several coiling shapes in *Mimagoniatites fecundus*. Such developmental plasticity likely played a role in the rapid radiation of the early ammonoids.

Several models for the development of the embryonic shell of ammonoids have been proposed (see Landman et al., 1996). These models feature opposing views. Either the ammonitella was calcified in its entirety (Bandel, 1982; Tanabe, 1989) or it was accreted as small increments at the aperture as in the adult shell (Erben, 1964b, 1966; Erben et al., 1968; Tanabe, 1989). The data presented here do not suggest a good fit with either of these views. The presence of transverse lirae has been used as evidence for an accretionary mode of formation (Erben, 1964b, 1966; Tanabe, 1989), with growth occurring at the apertural edge in small increments followed by hiatuses, producing growth lines (Bucher et al., 1996). The transverse lirae are not growth lines (Bucher et al., 2003) and no growth lines appear between lirae on the embryonic shell. The marginal accretionary mode of formation would likely result in a regular spacing as the mantle edge moved forward in small increments. The distance between any two consecutive lirae on the venter should be proportional to the distance between the same lirae on the dorsum. This is not what is observed for these primitive ammonoids. The V/D ratio shows wide fluctuations between consecutive lirae (Fig. 2.6c, d).

Other models for ammonitella formation suggest a nonaccretionary mode of formation (Bandel, 1982; Tanabe, 1989). The presence of the "wrinkle-like" creases between the transverse lirae suggest an organic component. The production of an organic nonmineralized shell eliminates the need for the lirae to be produced in an even fashion and the V/D ratio could then vary. This might also explain the differences in shape observed by Erben (1950) in the coiling of the ammonitella of *Mimagoniatites fecundus*. There is also no need for the entire nonmineralized shell to calcify simultaneously. Stepwise growth at the aperture has been observed in molluscs during the formation of large scale ornamental features (Vermeij, 1993). And similar models have been proposed for ammonoids (Checa, 1995; Bucher et al., 2003). While neither of these models produces ornament like that on these embryonic shells, it does suggest that ammonoids have the ability to produce the shell wall in a variety of ways, including growing short segments of organic material, and then calcifying it. This would also account for the fluctuations in the spacing observed if the segments produced were from lira to lira.

The models proposed for ammonitella formation are based, at least in part, on the embryonic development of extant taxonomic groups. Nonaccretionary models rely heavily on archaeogastropod developmental models (Bandel, 1982) and accretionary models on *Nautilus* development (Arnold et al., 1987). The embryonic shell of *Nautilus* grows by forward accretion at the aperture (Arnold et al., 1987). It produces a reticulate ornament with both longitudinal and transverse elements strongly developed. A similar ornament has been described in some Jurassic nautilids (Chirat and von Boletzky, 2003). This ornament is different from that described for Devonian ammonoids. The transverse elements in the nautilids appear as if imbricated and the longitudinal elements are not the "wrinkle-like" creases described here, but rather strongly developed longitudinal ridges that intersect the transverse lines. While examining related modern taxa is useful, the phylogenetic distance of these taxa must also be considered (Jacobs and Landman, 1993). The Nautiloidea lie some distance away from the Ammonoidea (Berthold and Engeser, 1987; Engeser, 1990, 1996). Furthermore, between the nautiloids and the three families in this study lie several taxonomic groups (Orthocerida, Bactritida, and several more basal ammonoid families, see Becker and Kullmann, 1996; Korn and Klug, 2002) several of which have distinctly different embryonic shells [see Doguzhaeva (1996a, b, 2002) for the bactritids and Ristedt (1968) for the orthocerids]. While data do exist for more basal ammonoid taxa (Sandberger, 1851; Schindewolf, 1933; Erben, 1950, 1960, 1962, 1964b, 1965; Chlupáč and Turek, 1983), they are scarce and the material is not as well preserved. Due to the open nature of their coiling, the inner whorls are often lost, and when they are preserved, they are often steinkerns. The external morphology of the shell is necessary for comparison. What is known is that members of one clade (the Agoniatitida) show remarkable variation at a very early developmental stage. Such developmental plasticity very early in ontogeny may have aided the rapid radiation of the ammonoids in the Devonian.

## 5 Conclusions

While still limited by a small number of specimens (seven), this study has added data to our understanding of the nature of and differences between three closely related families of early ammonoids. This study has confirmed a previous finding on the nature of the aperture of the ammonitella (Klofak et al., 1996). In both the Mimagoniatitidae and the Anarcestidae there is no primary varix. Furthermore, there is a suggestion that the absence of a varix produces a weak aperture, which is prone to breakage.

The Mimagoniatitidae, the Anarcestidae, and the Agoniatitidae all possess the same ornament, i.e., transverse lirae with longitudinal "wrinkle-like" creases stretched between them. However, the degree to which these "wrinkle-like" creases are expressed is different for the three families. The number of the lirae is also different for the three families. Most of the difference can be found on the initial chamber.

Other differences between these families can be seen in the pattern of the distances between the lirae on the ammonitella, especially on the initial chamber. In the Mimagoniatitidae, the changes in the spacing of the lirae follow the same pattern on both the ventral and dorsal sides of the shell. In the Anarcestidae and the Agoniatitidae, the pattern of change is different for the ventral and dorsal sides of the shell. In the Anarcestidae, where the ventral part of the shell shows an increase in the distance between lirae, the dorsal part of the shell shows no change or a slight decrease. And in the Agoniatitidae we see an increase in distance between the lirae on the ventral part of the shell, while there is a decrease on the dorsal part of the shell. The end of the initial chamber is marked, as in the Mimagoniatitidae and the Anarcestidae, by a decrease in the distance between lirae. This decrease provides a method of defining the limits of the initial chamber based on a character present at its formation, rather than a character added later in embryonic development as is currently used (the first suture). This makes better biological sense.

## Acknowledgments

The authors would like to thank the following people: Kathy B. Sarg for helping with work on the SEM; Jacob Mey and Kevin Frischman for making sure everything worked right with the SEM; Steve Thurston for helping with photography and graphics; Ilya Temkin for translating Russian papers; and Stephanie Crooms, Bushra Hussaini, Kristin Polizzotto, and Yumiko Iwasaki for a variety of formatting and typing issues. Thanks are also extended to Michael House, Thomas Becker, Christian Klug, Bruno Fectay, Yumiko Iwasaki, and Kathy B. Sarg for assistance doing fieldwork in Morocco. Kazushige Tanabe, Roger Hewitt, and Christian Klug are thanked for editorial comments and Ed Landing for allowing us to examine New York material. This research was funded by the Norman D. Newell Fund for Invertebrate Paleontology at the AMNH and the Lerner-Gray Fund for Marine Research to S. M. Klofak at the AMNH.

## Appendix 1

Lirae spacing (in microns) on the embryonic shell of *Archanarcestes obesus* (AMNH 45370).

| Lirae space number | Ventral (V) | Midflank | Dorsal (D) | Ratio V/D |
|---|---|---|---|---|
| 1 | | 32.6 | | |
| 2 | 32.6 | 32.4 | 28.0 | 1.2 |
| 3 | 36.8 | 31.0 | 24.8 | 1.5 |
| 4 | 38.6 | 35.6 | 31.6 | 1.2 |
| 5 | 40.0 | 34.6 | 27.0 | 1.5 |
| 6 | 40.6 | 33.2 | 23.4 | 1.7 |
| 7 | 48.2 | 40.6 | | |
| 8 | 57.0 | 50.8 | | |
| 9 | 58.0 | 49.0 | | |
| 10 | 63.2 | 52.8 | | |
| 11 | 46.4 | 40.4 | | |
| 12 | 53.8 | | | |

(continued)

(continued)

| Lirae space number | Ventral (V) | Midflank | Dorsal (D) | Ratio V/D |
|---|---|---|---|---|
| 13 | 42.6 | | | |
| 14 | 39.6 | | | |
| 15 | 36.8 | | | |
| 16 | 39.4 | | | |
| 17 | 33.0 | | | |
| 18 | 34.6 | | | |
| 19 | 37.0 | | | |
| 20 | 34.8 | | | |
| 21 | 38.8 | | | |
| 22 | 38.8 | | | |
| 23 | 32.2 | | | |
| 24 | 24.4 | 19.8 | 7.2 | 3.4 |
| 25 | 25.6 | 12.4 | 6.2 | 4.1 |
| 26 | 30.8 | 20.6 | 11.6 | 2.7 |
| 27 | 35.4 | 18.6 | 12.0 | 2.9 |
| 28 | 32.2 | 27.4 | 12.0 | 2.7 |
| 29 | 33.8 | 26.4 | 16.8 | 2.0 |
| 30 | 35.6 | 25.0 | 13.4 | 2.7 |
| 31 | 33.0 | 29.0 | 18.0 | 1.8 |
| 32 | 46.0 | 33.2 | 18.8 | 2.5 |
| 33 | 45.0 | 35.0 | 17.0 | 2.7 |
| 34 | 38.4 | 33.2 | 19.0 | 2.0 |
| 35 | 39.2 | 32.2 | 20.8 | 1.9 |
| 36 | 39.0 | 37.0 | 22.6 | 1.7 |
| 37 | 17.8 | 14.2 | 11.4 | 1.6 |
| 38 | 24.6 | 21.2 | 12.6 | 2.0 |
| 39 | 40.2 | 28.6 | 24.2 | 1.7 |
| 40 | 39.6 | 30.6 | 21.6 | 1.8 |
| 41 | 42.2 | 32.0 | 19.2 | 2.2 |
| 42 | 41.2 | 33.4 | 23.2 | 1.8 |
| 43 | 42.6 | 34.0 | 21.8 | 2.0 |
| 44 | 51.2 | 36.8 | 20.0 | 2.6 |
| 45 | 45.2 | 34.6 | 22.4 | 2.0 |
| 46 | 41.0 | 29.2 | 23.8 | 1.7 |
| 47 | 41.4 | 28.8 | 20.6 | 2.0 |
| 48 | 44.6 | 31.0 | 22.4 | 2.0 |
| 49 | 46.2 | 35.4 | 21.2 | 2.2 |
| 50 | 49.8 | 32.8 | 21.6 | 2.3 |
| 51 | 39.0 | 31.0 | 20.4 | 1.9 |
| 52 | 37.0 | 31.6 | 21.2 | 1.8 |
| 53 | 42.4 | 32.4 | 28.0 | 1.5 |
| 54 | 43.0 | 35.8 | 17.8 | 2.4 |
| 55 | 41.4 | 33.0 | 16.8 | 2.5 |
| 56 | 46.0 | 32.4 | 17.8 | 2.6 |
| 57 | 46.4 | 32.8 | 19.6 | 2.4 |
| 58 | 51.6 | 31.8 | 18.2 | 2.8 |

(continued)

(continued)

| Lirae space number | Ventral (V) | Midflank | Dorsal (D) | Ratio V/D |
|---|---|---|---|---|
| 59 | 45.4 | 32.8 | 19.8 | 2.3 |
| 60 | 28.8 | 18.2 | 12.2 | 2.4 |
| 61 | 26.4 | 19.6 | 12.2 | 2.2 |
| 62 | 6.9 | 6.6 | 5.1 | 1.4 |
| 63 | 8.4 | 7.7 | | |
| 64 | 7.5 | 6.1 | | |
| 65 | 8.8 | 8.1 | | |
| 66 | 20.3 | 16.1 | | |
| 67 | 23.4 | 10.1 | | |
| 68 | 8.4 | | | |
| 69 | 7.5 | | | |

# Appendix 2

Lirae spacing (in microns) on the embryonic shell of *Archanarcestes obesus* (AMNH 45374).

| Lirae space number | Ventral (V) | Midflank | Dorsal (D) | Ratio V/D |
|---|---|---|---|---|
| 1 | 35.1 | 35.1 | 28.0 | 1.2 |
| 2 | 49.8 | 49.5 | 41.9 | 1.2 |
| 3 | 53.3 | 43.0 | 32.7 | 1.6 |
| 4 | 43.0 | 37.3 | | |
| 5 | 43.1 | 37.1 | 35.0 | 1.2 |
| 6 | 40.1 | 42.5 | 28.9 | 1.4 |
| 7 | 35.2 | 34.8 | 24.1 | 1.5 |
| 8 | 33.4 | 32.5 | 26.2 | 1.3 |
| 9 | 31.3 | 34.7 | 25.1 | 1.3 |
| 10 | 35.7 | 30.1 | 25.2 | 1.4 |
| 11 | 35.9 | 32.0 | 27.2 | 1.3 |
| 12 | 46.2 | 40.2 | 26.8 | 1.7 |
| 13 | 63.4 | 49.6 | 25.9 | 2.5 |
| 14 | 42.6 | 39.9 | 31.7 | 1.3 |
| 15 | 48.4 | 40.0 | 25.9 | 1.2 |
| 16 | 48.4 | 37.8 | 25.2 | 1.9 |
| 17 | 46.5 | 37.0 | 27.3 | 1.7 |
| 18 | 37.0 | 29.8 | 21.3 | 1.7 |
| 19 | 35.5 | 23.2 | 19.3 | 1.8 |
| 20 | 30.9 | 21.8 | 14.3 | 2.2 |
| 22 | 19.6 | | | |
| 23 | 9.6 | | | |
| 24 | 11.2 | | | |
| 25 | 17.6 | 14.0 | 10.2 | 1.7 |
| 26 | 21.4 | 18.0 | 8.0 | 2.7 |
| 27 | 27.2 | 15.8 | 12.4 | 2.2 |

(continued)

(continued)

| Lirae space number | Ventral (V) | Midflank | Dorsal (D) | Ratio V/D |
|---|---|---|---|---|
| 28 | 36.0 | 18.2 | 8.6 | 4.2 |
| 29 | 37.6 | 20.4 | 11.8 | 3.2 |
| 30 | 28.0 | 27.4 | 11.8 | 2.1 |
| 31 | 38.4 | 30.0 | 22.2 | 1.7 |
| 32 | 42.2 | 31.2 | 24.8 | 1.7 |
| 33 | 32.8 | 30.4 | 24.0 | 1.4 |
| 34 | 38.2 | 26.8 | 23.0 | 1.7 |
| 35 | 48.3 | 38.6 | 24.6 | 2.0 |
| 36 | 47.6 | 36.6 | 23.2 | 2.1 |
| 37 | 47.0 | 42.4 | 22.8 | 2.1 |
| 38 | 47.2 | 36.4 | 20.6 | 2.3 |
| 39 | | | 22.4 | |
| 40 | | | 19.2 | |
| 41 | | | 19.2 | |
| 42 | 33.0 | | | |
| 43 | 42.6 | | | |
| 44 | 38.2 | | | |
| 45 | 40.0 | | 23.0 | 1.7 |
| 46 | 37.4 | 30.6 | 22.8 | 1.6 |
| 47 | 39.8 | 33.4 | 21.4 | 1.9 |
| 48 | 35.0 | 29.2 | 17.4 | 2.0 |
| 49 | 23.6 | 20.0 | 12.0 | 2.0 |
| 50 | 43.8 | 32.8 | 26.4 | 1.7 |
| 51 | 54.4 | 42.4 | 28.4 | 1.9 |
| 52 | 45.6 | 36.2 | 32.2 | 1.4 |
| 53 | 53.2 | 40.6 | 31.0 | 1.7 |
| 54 | 56.8 | 33.2 | 24.4 | 2.3 |
| 55 | | 28.2 | 22.0 | |
| 56 | | 23.2 | 19.0 | |
| 57 | | 19.6 | 16.8 | |
| 58 | | 37.2 | 34.2 | |
| 59 | | 25.6 | 18.6 | |
| 60 | 38.6 | 31.4 | 38.2 | 1.0 |
| 61 | 40.8 | | | |
| 62 | 24.2 | | | |
| 63 | 42.2 | | | |
| 64 | 37.2 | | | |
| 65 | 34.8 | | | |
| 66 | 28.6 | | | |
| 67 | 25.0 | | | |
| 68 | 27.6 | | | |
| 69 | 28.4 | | | |
| 70 | 25.4 | | | |
| 71 | 26.6 | | | |
| 72 | 25.6 | | | |
| 73 | 24.6 | | | |

(continued)

(continued)

| Lirae space number | Ventral (V) | Midflank | Dorsal (D) | Ratio V/D |
|---|---|---|---|---|
| 74 | 23.6 | | | |
| 75 | 27.8 | | | |
| 76 | 23.6 | | | |
| 77 | 23.0 | | | |
| 78 | 24.0 | | | |

# Appendix 3

Lirae spacing (in microns) on the postembryonic shell of *Archanarcestes obesus* (AMNH 45374).

| Lirae space number | Ventral (V) | Midflank | Dorsal (D) | Ratio V/D |
|---|---|---|---|---|
| 1 | 54.8 | 56.0 | 56.0 | 1.0 |
| 2 | 36.0 | 26.2 | 32.4 | 1.1 |
| 3 | 75.0 | 50.4 | 32.0 | 2.3 |
| 4 | 52.6 | 39.2 | 34.6 | 1.5 |
| 5 | 67.4 | 58.6 | 48.8 | 1.4 |
| 6 | | | 59.0 | |
| 7 | | | 47.6 | |
| 8 | | | 45.2 | |
| 9 | 68.2 | | 33.4 | 2.0 |
| 10 | 74.6 | 54.2 | 34.4 | 2.2 |
| 11 | 82.0 | 62.4 | 53.2 | 1.5 |
| 12 | | | 66.4 | |
| 13 | | | 63.4 | |
| 14 | | | 63.4 | |
| 15 | | | 65.6 | |
| 16 | | | 63.6 | |
| 17 | | 72.6 | 64.8 | |
| 18 | | | 67.2 | |
| 19 | | | 62.6 | |
| 20 | | 66.2 | 67.2 | |
| 21 | | 82.4 | 66.2 | |
| 22 | | 99.2 | 71.2 | |
| 23 | | | 54.0 | |
| 24 | | 67.4 | 53.2 | |
| 25 | | 71.2 | 53.2 | |
| 26 | | 79.8 | 54.8 | |
| 27 | | 80.4 | 70.0 | |
| 28 | | 73.4 | 60.8 | |
| 29 | | 87.8 | 71.8 | |
| 30 | | 96.4 | 78.8 | |
| 31 | | 115.8 | 93.8 | |

(continued)

# Appendix 4

Lirae spacing (in microns) on the embryonic shell of *Mimagoniatites fecundus* (AMNH 46645).

| Lirae space number | Ventral (V) | Midflank | Dorsal (D) | Ratio V/D |
|---|---|---|---|---|
| 1 | | 14.2 | | |
| 2 | 16.6 | 17.4 | | |
| 3 | 26.9 | 16.6 | | |
| 4 | 28.4 | 27.7 | | |
| 5 | 35.6 | 21.2 | 23.7 | 1.6 |
| 6 | 26.9 | 18.2 | 10.3 | 2.6 |
| 7 | 26.1 | 34.0 | 10.3 | 2.5 |
| 8 | 44.2 | 28.4 | 12.6 | 3.5 |
| 9 | 49.0 | 31.6 | 10.3 | 4.8 |
| 10 | 54.5 | 30.8 | 8.7 | 6.3 |
| 11 | 55.3 | 42.7 | 15.0 | 3.7 |
| 12 | 64.8 | 45.8 | 9.5 | 6.8 |
| 13 | 70.3 | 49.0 | 11.9 | 5.9 |
| 14 | 69.5 | 49.0 | 19.8 | 3.5 |
| 15 | 66.4 | 50.6 | 15.8 | 4.2 |
| 16 | 75.1 | 54.5 | 28.4 | 2.6 |
| 17 | 64.8 | 57.7 | 19.8 | 3.3 |
| 18 | 66.4 | 52.1 | 27.7 | 2.4 |
| 19 | 62.4 | 58.5 | 26.9 | 2.3 |
| 20 | 63.2 | 49.0 | 25.3 | 2.5 |
| 21 | 66.4 | 53.7 | 22.1 | 3.0 |
| 22 | 64.0 | 50.6 | 23.7 | 2.7 |
| 23 | 64.0 | 52.1 | 23.7 | 2.7 |
| 24 | 66.4 | 42.7 | 22.1 | 3.1 |
| 25 | 72.7 | 48.2 | 19.0 | 3.8 |
| 26 | 85.2 | 42.7 | 18.2 | 3.7 |
| 27 | 54.5 | 36.3 | 19.8 | 2.8 |
| 28 | 48.2 | 34.0 | 19.8 | 2.4 |
| 29 | 56.1 | 38.7 | 15.0 | 3.7 |
| 30 | 54.5 | 31.6 | 20.5 | 2.7 |
| 31 | 58.5 | 37.1 | 16.6 | 3.5 |
| 32 | 48.2 | 35.6 | 15.8 | 3.1 |
| 33 | 62.4 | 52.1 | 27.1 | 2.4 |
| 34 | 86.3 | 67.9 | 41.1 | 2.1 |
| 35 | 75.1 | 56.1 | 39.5 | 1.9 |
| 36 | 75.1 | 59.3 | 45.0 | 1.7 |
| 37 | 90.1 | 69.5 | 44.2 | 2.0 |
| 38 | 111.4 | 71.1 | 50.6 | 2.2 |
| 39 | 92.4 | 71.1 | 26.9 | 3.4 |
| 40 | 83.0 | 65.6 | 35.5 | 2.3 |
| 41 | 90.9 | 62.4 | 35.5 | 2.6 |
| 42 | 101.9 | 60.8 | 37.1 | 2.7 |

(continued)

(continued)

| Lirae space number | Ventral (V) | Midflank | Dorsal (D) | Ratio V/D |
|---|---|---|---|---|
| 43 | 98.0 | 71.9 | 41.1 | 2.3 |
| 44 | 96.4 | 74.3 | 42.7 | 2.8 |
| 45 | 92.4 | 71.1 | 34.8 | 2.7 |
| 46 | 101.9 | 74.3 | 30.0 | 3.4 |
| 47 | 102.7 | 59.3 | 31.6 | 3.3 |
| 48 | 83.7 | 54.5 | 26.9 | 2.9 |
| 49 | 124.0 | 64.8 | 30.0 | 4.1 |
| 50 | 93.2 | 57.7 | 36.3 | 2.6 |
| 51 | 97.2 | 64.0 | 29.2 | 3.3 |
| 52 | 65.6 | 47.4 | 25.3 | 2.6 |
| 53 | 52.1 | 46.6 | 24.5 | 2.1 |
| 54 | 57.7 | 42.7 | 23.7 | 2.4 |
| 55 | 79.0 | 64.8 | 25.3 | 3.1 |
| 56 | 80.6 | 48.2 | 20.5 | 3.9 |
| 57 | | 49.8 | 15.8 | |
| 58 | | 44.2 | 13.4 | |
| 59 | | 45.0 | 17.4 | |
| 60 | 60.0 | 39.5 | 18.2 | 3.3 |
| 61 | 45.0 | 47.4 | 11.1 | 4.1 |
| 62 | 57.7 | 45.0 | 14.2 | 4.1 |
| 63 | 63.2 | 49.0 | 11.9 | 5.3 |
| 64 | 58.5 | 43.5 | 15.0 | 3.9 |
| 65 | 59.3 | 42.7 | 16.6 | 3.6 |
| 66 | 60.8 | 49.8 | 25.3 | 2.4 |
| 67 | 79.8 | 75.8 | 28.4 | 2.8 |
| 68 | 33.2 | 24.5 | 15.0 | 2.2 |
| 69 | 37.9 | 35.6 | 14.2 | 2.7 |
| 70 | 37.1 | 30.8 | 14.2 | 2.6 |
| 71 | 57.7 | 34.8 | 14.2 | 4.1 |
| 72 | 62.4 | 43.5 | 18.2 | 3.4 |
| 73 | 49.0 | 45.0 | 16.6 | 3.0 |
| 74 | 34.8 | 26.9 | 13.4 | 2.6 |
| 75 | 31.6 | 22.1 | 19.8 | 1.6 |
| 76 | | 17.4 | | |

# Appendix 5

Lirae spacing (in microns) on the postembryonic shell of *Mimagoniatites fecundus* (AMNH 46645).

| Lirae space number | Ventral (V) | Midflank | Dorsal (D) | Ratio V/D |
|---|---|---|---|---|
| 1 | 29.2 | 15.0 | 31.6 | 0.9 |
| 2 | 30.8 | 9.5 | 28.4 | 1.1 |
| 3 | 46.6 | 3.2 | 42.7 | 1.1 |
| 4 | 37.1 | 30.0 | 22.1 | 1.7 |
| 5 | 36.3 | 23.7 | 26.1 | 1.4 |
| 6 | 42.7 | 44.2 | 29.2 | 1.5 |
| 7 | 57.7 | 49.0 | 36.3 | 1.6 |
| 8 | 41.1 | 43.5 | 29.2 | 1.4 |
| 9 | 42.7 | 45.0 | 25.3 | 1.7 |
| 10 | 67.2 | 48.2 | 37.9 | 1.8 |
| 11 | 86.9 | 68.7 | 45.0 | 1.9 |
| 12 | 69.5 | 60.0 | 48.2 | 1.4 |
| 13 | 83.7 | 55.3 | 38.7 | 2.2 |
| 14 | 84.5 | 52.9 | 39.5 | 2.1 |
| 15 | 56.1 | 50.6 | 39.5 | 1.4 |
| 16 | 59.3 | 58.5 | 34.8 | 1.7 |
| 17 | 65.6 | 48.2 | 38.7 | 1.7 |
| 18 | 60.8 | 57.7 | 34.0 | 1.8 |
| 19 | 67.9 | 62.4 | 48.2 | 1.4 |
| 20 | 67.2 | 61.6 | 40.3 | 1.7 |
| 21 | 108.2 | 72.7 | 51.4 | 1.7 |
| 22 | 78.2 | 31.6 | 6.3 | 12.4 |
| 23 | 90.1 | 71.1 | 54.5 | 1.7 |
| 24 | 94.0 | 65.6 | 52.9 | 1.8 |
| 25 | 78.2 | 71.1 | 55.3 | 1.4 |
| 26 | 80.6 | 67.2 | 43.5 | 1.9 |
| 27 | 65.6 | 56.9 | 37.1 | 1.8 |
| 28 | 102.7 | 61.6 | 47.4 | 2.2 |
| 29 | 113.0 | 78.2 | 74.3 | 1.5 |
| 30 | 104.3 | 131.1 | 46.6 | 2.2 |
| 31 | 106.7 | 83.7 | 59.3 | 1.8 |
| 32 | 143.0 | 129.6 | 85.3 | 1.7 |
| 33 | 122.5 | 108.2 | 56.9 | 2.2 |
| 34 | 99.5 | 64.0 | 52.1 | 1.9 |
| 35 | 105.1 | 91.6 | 65.6 | 1.6 |
| 36 | 83.7 | 56.1 | | |
| 37 | 93.2 | 73.5 | | |
| 38 | 91.6 | 64.0 | | |
| 39 | 88.5 | 71.9 | | |
| 40 | 109.8 | 79.8 | 67.9 | 1.6 |
| 41 | 216.5 | 122.5 | 87.7 | 2.5 |
| 42 | 109.8 | 116.9 | 83.0 | 1.3 |

(continued)

(continued)

| Lirae space number | Ventral (V) | Midflank | Dorsal (D) | Ratio V/D |
|---|---|---|---|---|
| 43 | 110.6 | 103.5 | 67.2 | 1.7 |
| 44 | 142.2 | 90.9 | 58.5 | 2.5 |
| 45 | 116.1 | 94.8 | 73.5 | 1.6 |
| 46 | 120.9 | 96.4 | 69.5 | 1.7 |
| 47 | 169.9 | 122.5 | 86.1 | 2.0 |
| 48 | 110.6 | 78.2 | | |
| 49 | 93.2 | 84.5 | | |
| 50 | 124.8 | 92.4 | | |
| 51 | | 95.6 | | |
| 52 | | 96.4 | | |
| 53 | | 88.5 | | |
| 54 | | 43.5 | | |
| 55 | | 87.7 | | |

# Appendix 6

Lirae spacing (in microns) on the embryonic shell of *Latanarcestes* sp. (AMNH 46646).

| Lirae space number | Ventral (V) | Midflank | Dorsal (D) | Ratio V/D |
|---|---|---|---|---|
| 1 | 15.8 | 16.8 | 7.9 | 2.0 |
| 2 | 16.8 | 16.8 | 8.9 | 1.9 |
| 3 | 17.8 | 16.8 | 11.9 | 1.4 |
| 4 | 27.7 | 21.7 | 16.8 | 1.7 |
| 5 | 29.6 | 24.7 | 16.8 | 1.8 |
| 6 | 24.7 | 26.7 | 17.8 | 1.4 |
| 7 | 26.7 | 27.7 | 13.8 | 1.9 |
| 8 | 28.7 | 24.7 | 16.8 | 1.7 |
| 9 | 24.7 | 27.7 | 13.8 | 1.8 |
| 10 | 28.7 | 28.7 | 19.8 | 1.5 |
| 11 | 32.6 | 29.6 | 15.8 | 2.1 |
| 12 | 29.6 | 25.7 | 13.8 | 2.1 |
| 13 | 36.6 | 31.6 | 12.8 | 2.9 |
| 14 | 36.6 | 26.7 | 14.8 | 2.5 |
| 15 | 33.6 | 31.6 | 13.8 | 2.4 |
| 16 | 35.6 | 29.6 | 8.9 | 4.0 |
| 17 | 32.6 | 25.7 | 11.9 | 2.8 |
| 18 | 35.6 | 28.7 | 13.8 | 2.6 |
| 19 | 38.5 | 32.6 | 9.9 | 3.9 |
| 20 | 35.6 | 30.6 | 7.9 | 4.5 |
| 21 | 38.5 | 32.6 | 13.8 | 2.8 |
| 22 | 40.5 | 34.6 | 14.8 | 2.6 |

(continued)

(continued)

| Lirae space number | Ventral (V) | Midflank | Dorsal (D) | Ratio V/D |
|---|---|---|---|---|
| 23 | 39.5 | 32.6 | 10.9 | 3.6 |
| 24 | 39.5 | 31.6 | 10.9 | 3.6 |
| 25 | 45.5 | 31.6 | 7.9 | 5.8 |
| 26 | 44.5 | 32.6 | 7.9 | 5.6 |
| 27 | 52.4 | 31.6 | 4.9 | 10.6 |
| 28 | 45.5 | 34.6 | 8.9 | 5.1 |
| 29 | 48.4 | 34.6 | 4.9 | 9.8 |
| 30 | 59.3 | 31.6 | 6.9 | 8.6 |
| 31 | 52.4 | 27.7 | 10.0 | 5.3 |
| 32 | 59.3 | 27.7 | 5.9 | 10.0 |
| 33 | 42.5 | 23.7 | 4.0 | 10.8 |
| 34 | 51.4 | 31.6 | 6.9 | 7.4 |
| 35 | 58.3 | 33.6 | | |
| 36 | 42.5 | 36.6 | | |
| 37 | 58.3 | 35.6 | | |
| 38 | 34.6 | 27.7 | | |
| 39 | 39.5 | 22.7 | | |
| 40 | 35.6 | 18.8 | | |
| 41 | 33.6 | 21.7 | | |
| 42 | 35.6 | 17.8 | | |
| 43 | 30.6 | 19.8 | | |
| 44 | 27.7 | 17.8 | | |
| 45 | 42.5 | 20.8 | | |
| 46 | 41.5 | 27.7 | | |
| 47 | 40.5 | 21.7 | | |
| 48 | 49.4 | 33.6 | | |
| 49 | 48.4 | 40.5 | | |
| 50 | 53.4 | 25.7 | | |
| 51 | 51.4 | 34.6 | | |
| 52 | 50.4 | 32.6 | | |
| 53 | 45.5 | 33.6 | | |
| 54 | 43.5 | 23.7 | | |
| 55 | 20.8 | 21.7 | | |
| 56 | 38.5 | 38.5 | | |
| 57 | 82.0 | 70.2 | | |
| 58 | 83.0 | 65.2 | | |
| 59 | 70.2 | 54.3 | | |
| 60 | 56.3 | 43.5 | | |
| 61 | 50.4 | 38.5 | | |
| 62 | 40.5 | 37.5 | | |
| 63 | 51.4 | 43.5 | | |
| 64 | 51.4 | 35.6 | | |
| 65 | 61.3 | | | |
| 66 | 59.3 | | | |
| 67 | 42.5 | | | |

(continued)

(continued)

| Lirae space number | Ventral (V) | Midflank | Dorsal (D) | Ratio V/D |
|---|---|---|---|---|
| 68 | 50.4 | | | |
| 69 | 62.2 | | | |
| 70 | 37.5 | | | |
| 71 | 35.6 | | | |
| GAP | | | | |
| 80 | 34.6 | | | |
| 81 | 25.7 | | | |
| 82 | 16.8 | | | |
| 83 | 24.7 | | | |
| 84 | 17.8 | | | |
| 85 | | | | |
| 86 | | | | |
| 87 | 24.7 | | | |
| 88 | 18.8 | | | |
| 89 | 21.7 | | | |
| 90 | 20.8 | 16.8 | | |
| 91 | 22.7 | 19.8 | | |
| 92 | 23.7 | 16.8 | | |
| 93 | 12.8 | 13.8 | | |
| 94 | 8.9 | 11.9 | | |
| 95 | 8.9 | 8.9 | | |

# Appendix 7

Lirae spacing (in microns) on the postembryonic shell of *Latanarcestes* sp. (AMNH 46646).

| Lirae space number | Ventral (V) | Midflank | Dorsal (D) | Ratio V/D |
|---|---|---|---|---|
| 1 | 10.0 | 19.8 | | |
| 2 | 10.9 | 13.8 | | |
| 3 | 10.9 | 15.8 | | |
| 4 | 8.9 | 11.9 | | |
| 5 | 15.8 | 11.9 | | |
| 6 | 32.6 | 18.8 | | |
| 7 | 46.4 | 36.6 | | |
| 8 | 46.4 | 29.6 | | |
| 9 | 37.5 | 28.7 | | |
| 10 | 36.6 | 27.7 | | |
| 11 | 31.6 | 24.7 | | |
| 12 | 33.6 | 32.6 | | |
| 13 | 34.6 | 29.6 | | |
| 14 | 38.5 | 31.6 | | |
| 15 | 42.5 | 42.5 | | |
| 16 | 49.4 | 50.4 | | |

(continued)

(continued)

| Lirae space number | Ventral (V) | Midflank | Dorsal (D) | Ratio V/D |
|---|---|---|---|---|
| 17 | 52.4 | 45.5 | | |
| 18 | 34.6 | 38.5 | 23.7 | 1.5 |
| 19 | 23.7 | 30.6 | 29.6 | 0.8 |
| 20 | 40.5 | 31.6 | 27.7 | 1.5 |
| 21 | 36.6 | 32.6 | 23.7 | 1.5 |
| 22 | 34.5 | 35.6 | 19.8 | 1.8 |
| 23 | 29.6 | 25.7 | 21.7 | 1.4 |
| 24 | 42.5 | 39.5 | 26.7 | 1.6 |
| 25 | 58.3 | 47.4 | 37.5 | 1.6 |
| 26 | 62.2 | 45.5 | 32.6 | 1.9 |
| 27 | 67.2 | 42.5 | 35.6 | 1.9 |
| 28 | 54.3 | 43.5 | 36.6 | 1.5 |
| 29 | 52.4 | 44.5 | 30.6 | 1.7 |
| 30 | 49.4 | 39.5 | 32.6 | 1.5 |
| 31 | 37.5 | 30.6 | 27.7 | 1.4 |
| 32 | 47.4 | 34.6 | 26.7 | 1.7 |
| 33 | 44.5 | 36.6 | 36.6 | 1.2 |
| 34 | 55.3 | 56.3 | 55.3 | 1.0 |
| 35 | 44.5 | 42.5 | 36.6 | 1.2 |
| 36 | 30.6 | 29.6 | 23.7 | 1.3 |
| 37 | 30.6 | 25.7 | 22.7 | 1.4 |
| 38 | 36.6 | 28.7 | 17.8 | 2.1 |
| 39 | 22.7 | 21.7 | 12.8 | 1.8 |
| 40 | 42.5 | 32.6 | 27.7 | 1.5 |
| 41 | 46.4 | 41.5 | 36.6 | 1.3 |
| 42 | 63.2 | 58.3 | 59.3 | 1.1 |
| 43 | 57.3 | 52.4 | 37.5 | 1.5 |
| 44 | 54.3 | 38.5 | 30.6 | 1.7 |
| 45 | 114.6 | 91.9 | 64.2 | 1.8 |
| 46 | 91.9 | 29.0 | 75.1 | 1.2 |
| 47 | 121.5 | 109.7 | 80.0 | 1.5 |
| 48 | 40.5 | 40.5 | 33.6 | 1.2 |

# Appendix 8

Lirae spacing (in microns) on the embryonic shell of *Latanarcestes* sp. (AMNH 50416).

| Lirae space number | Ventral (V) | Midflank | Dorsal (D) | Ratio V/D |
|---|---|---|---|---|
| 1 | 12.2 | 17.8 | 9.7 | 1.3 |
| 2 | 13.3 | 13.3 | 11.6 | 1.2 |
| 3 | 14.4 | 12.7 | 8.9 | 1.6 |
| 4 | 14.2 | 12.2 | 7.2 | 2.0 |
| 5 | 18.7 | 10.9 | 13.9 | 1.3 |

(continued)

(continued)

| Lirae space number | Ventral (V) | Midflank | Dorsal (D) | Ratio V/D |
|---|---|---|---|---|
| 6 | 16.9 | 14.8 | 8.8 | 1.9 |
| 7 | 21.3 | 12.6 | 10.0 | 2.1 |
| 8 | 25.3 | 14.8 | 12.4 | 2.0 |
| 9 | 18.9 | 14.6 | 11.2 | 1.7 |
| 10 | 23.1 | 12.0 | 7.3 | 3.2 |
| 11 | 19.1 | 15.4 | 10.9 | 1.8 |
| 12 | 22.3 | 14.9 | 11.8 | 1.9 |
| 13 | 25.3 | 14.2 | 6.4 | 4.0 |
| 14 | 28.8 | 20.5 | 9.5 | 3.0 |
| 15 | 28.6 | 18.5 | 10.2 | 2.8 |
| 16 | 25.2 | 21.4 | 8.8 | 2.9 |
| 17 | 22.5 | 17.7 | 10.0 | 2.3 |
| 18 | 16.5 | 15.3 | 12.8 | 1.3 |
| 19 | 16.5 | 13.3 | 5.7 | 2.9 |
| 20 | 28.8 | 10.5 | 8.8 | 3.3 |
| 21 | 23.7 | 16.9 | 12.2 | 1.9 |
| 22 | 30.9 | 19.2 | 10.4 | 3.0 |
| 23 | 34.1 | 19.2 | 10.7 | 3.2 |
| 24 | 26.7 | 22.9 | 10.1 | 2.6 |
| 25 | 25.6 | 18.0 | 8.2 | 3.1 |
| 26 | 23.3 | 20.4 | 7.7 | 3.0 |
| 27 | 22.9 | 18.3 | 7.0 | 3.3 |
| 28 | 24.0 | 17.4 | 9.5 | 2.5 |
| 29 | 25.8 | 15.4 | 8.8 | 2.9 |
| 30 | 28.5 | 20.5 | 6.9 | 4.1 |
| 31 | 23.1 | 16.3 | 8.7 | 2.8 |
| 32 | 24.7 | 18.6 | 8.3 | 3.0 |
| 33 | 23.3 | 14.9 | 6.4 | 3.6 |
| 34 | 24.7 | 18.0 | 5.6 | 4.4 |
| 35 | 25.4 | 14.8 | 5.6 | 4.5 |
| 36 | 28.2 | 12.5 | 7.1 | 4.0 |
| 37 | 24.2 | 14.0 | 5.6 | 4.3 |
| 38 | 20.3 | 10.7 | | |
| 39 | 23.8 | 12.6 | | |
| 40 | 15.6 | 12.9 | | |
| 41 | 16.1 | 10.4 | | |
| 42 | 19.7 | 13.9 | | |
| 43 | 22.2 | 10.1 | | |
| 44 | 17.3 | 10.7 | | |
| 45 | 27.9 | 13.8 | | |
| 46 | 26.5 | 14.3 | 7.6 | 3.5 |
| 47 | 38.7 | 14.4 | 7.3 | 5.3 |
| 48 | 24.9 | 18.3 | 8.4 | 3.0 |
| 49 | 24.7 | 16.1 | 6.2 | 4.0 |
| 50 | 20.3 | 21.3 | 4.4 | 4.6 |

(continued)

(continued)

| Lirae space number | Ventral (V) | Midflank | Dorsal (D) | Ratio V/D |
|---|---|---|---|---|
| 51 | 36.4 | 19.5 | 5.4 | 6.7 |
| 52 | 24.6 | 18.6 | 7.1 | 3.5 |
| 53 | 32.9 | 20.3 | 7.1 | 4.6 |
| 54 | 38.4 | 23.6 | 7.1 | 5.4 |
| 55 | 35.6 | 18.2 | 4.4 | 8.1 |
| 56 | 45.8 | 25.9 | 3.9 | 11.7 |
| 57 | 40.7 | 31.0 | 8.1 | 5.0 |
| 58 | 46.7 | 28.4 | 7.0 | 6.7 |
| 59 | 46.9 | 27.0 | 8.1 | 5.8 |
| 60 | 43.6 | 32.9 | 10.3 | 4.2 |
| 61 | 32.3 | 25.1 | 14.9 | 2.2 |
| 62 | 40.6 | 33.1 | 11.1 | 3.7 |
| 63 | 51.9 | 29.9 | 8.5 | 6.1 |
| 64 | 33.5 | 28.4 | 9.4 | 3.6 |
| 65 | 37.5 | 28.0 | 12.7 | 3.0 |
| 66 | 46.4 | 27.8 | 12.7 | 3.7 |
| 67 | 45.8 | 31.2 | 12.9 | 3.6 |
| 68 | 41.8 | 32.9 | 18.6 | 2.3 |
| 69 | 54.0 | 33.8 | 18.6 | 3.5 |
| 70 | 65.5 | 37.6 | 17.8 | 3.7 |
| 71 | 47.0 | 24.9 | 12.8 | 3.7 |
| 72 | 52.9 | 32.8 | 17.7 | 3.0 |
| 73 | 32.6 | 30.3 | 13.5 | 2.4 |
| 74 | 31.9 | 24.9 | 13.9 | 2.3 |
| 75 | 48.4 | 22.4 | 12.0 | 4.0 |
| 76 | 39.1 | 20.7 | 11.9 | 3.3 |
| 77 | 33.8 | 21.9 | 6.5 | 5.2 |
| 78 | 38.5 | 21.5 | 7.7 | 5.0 |
| 79 | 29.8 | 20.4 | 10.7 | 2.8 |
| 80 | 31.3 | 21.3 | 10.3 | 3.0 |
| 81 | 36.0 | 20.7 | 11.0 | 3.3 |
| 82 | 38.3 | 21.2 | 10.4 | 3.7 |
| 83 | 25.1 | 11.9 | 11.1 | 2.3 |
| 84 | 26.4 | 20.9 | 12.5 | 2.1 |
| 85 | 30.1 | 17.4 | 7.9 | 3.8 |
| 86 | 21.6 | 11.2 | 10.3 | 2.1 |
| 87 | 20.3 | 13.9 | 8.5 | 2.4 |
| 88 | 24.7 | 14.2 | 9.6 | 2.6 |
| 89 | 25.1 | 12.8 | 9.1 | 2.8 |
| 90 | 23.9 | 13.6 | 6.2 | 3.9 |
| 91 | 20.5 | 11.0 | | |
| 92 | 16.6 | 13.4 | | |
| 93 | 17.4 | 13.4 | | |
| 94 | 18.0 | 11.9 | 10.2 | 1.8 |
| 95 | | 10.2 | | |

## Appendix 9

Lirae spacing (in microns) on the postembryonic shell of *Latanarcestes* sp. (AMNH 50416).

| Lirae space number | Ventral (V) | Midflank | Dorsal (D) | Ratio V/D |
|---|---|---|---|---|
| 1 | 60.1 | 41.2 | 30.5 | 2.0 |
| 2 | 36.5 | 30.9 | 23.8 | 1.5 |
| 3 | 56.6 | 38.0 | 35.0 | 1.6 |
| 4 | 40.7 | 39.0 | 23.2 | 1.8 |
| 5 | 46.9 | 35.5 | 25.1 | 1.9 |
| 6 | 45.6 | 30.9 | 23.8 | 1.9 |
| 7 | 43.3 | 41.2 | 21.7 | 2.0 |
| 8 | 38.2 | 30.9 | 26.8 | 1.4 |
| 9 | 63.0 | 52.5 | 29.1 | 2.2 |
| 10 | 45.2 | 36.5 | 27.1 | 1.7 |
| 11 | 61.5 | 47.5 | 39.9 | 1.5 |
| 12 | 32.6 | 28.1 | 18.9 | 1.7 |
| 13 | 42.1 | 27.2 | 23.8 | 1.8 |
| 14 | 29.9 | 26.8 | 25.5 | 1.2 |
| 15 | 36.6 | 25.2 | 20.6 | 1.8 |
| 16 | 30.7 | 30.1 | 26.7 | 1.2 |
| 17 | 32.0 | 28.3 | 17.8 | 1.8 |
| 18 | 34.1 | 27.5 | 17.0 | 2.0 |
| 19 | 43.7 | 41.3 | 26.1 | 1.7 |
| 20 | 45.2 | 32.0 | 24.6 | 1.9 |
| 21 | 46.3 | 26.9 | 19.2 | 2.4 |
| 22 | | 25.5 | 20.1 | |

## Appendix 10

Lirae spacing (in microns) on the embryonic shell of *Agoniatites vanuxemi* (NYSM 3545).

| Lirae space number | Ventral (V) | Midflank | Dorsal (D) | Ratio V/D |
|---|---|---|---|---|
| 1 | 39.2 | 31.3 | 23.8 | 1.7 |
| 2 | 42.1 | 28.3 | 23.9 | 1.4 |
| 3 | 49.5 | 33.1 | 23.1 | 2.1 |
| 4 | 57.5 | 42.3 | 30.3 | 1.9 |
| 5 | 55.6 | 46.7 | 24.6 | 2.3 |
| 6 | 59.4 | 49.1 | 26.6 | 2.2 |
| 7 | 52.1 | 39.3 | 30.3 | 1.7 |
| 8 | 53.9 | 47.1 | 31.5 | 1.2 |
| 9 | 56.1 | 36.1 | 30.5 | 1.8 |
| 10 | 40.7 | 33.8 | 18.9 | 2.2 |
| 11 | 51.2 | 30.1 | 22.4 | 2.3 |

(continued)

(continued)

| Lirae space number | Ventral (V) | Midflank | Dorsal (D) | Ratio V/D |
|---|---|---|---|---|
| 12 | 49.6 | 44.4 | 19.8 | 2.5 |
| 13 | | 20.8 | | |
| 14 | | | | |
| 15 | | | 14.4 | |
| 16 | 41.4 | 27.4 | 16.9 | 2.5 |
| 17 | 43.0 | 29.4 | 20.3 | 2.1 |
| 18 | 56.9 | 37.0 | 13.3 | 4.2 |
| 19 | 36.0 | 30.5 | 16.1 | 5.9 |
| 20 | 57.5 | 37.9 | 13.3 | 4.3 |
| 21 | 52.8 | 31.7 | 14.8 | 3.6 |
| 22 | 49.3 | 33.9 | 12.1 | 4.1 |
| 23 | 42.0 | 38.1 | 13.0 | 3.2 |
| 24 | 57.0 | 42.1 | 17.5 | 3.3 |
| 25 | 50.0 | 41.4 | 17.4 | 2.9 |
| 26 | 53.4 | 35.8 | 20.3 | 2.6 |
| 27 | 59.1 | 34.2 | 22.7 | 2.6 |
| 28 | 66.1 | 38.2 | 17.0 | 3.9 |
| 29 | 55.9 | 31.8 | 24.3 | 2.3 |
| 30 | 64.6 | 30.7 | 15.4 | 4.2 |
| 31 | 58.7 | 33.4 | 14.4 | 4.1 |
| 32 | 61.9 | 36.8 | 13.5 | 4.6 |
| 33 | 64.4 | 33.0 | 13.8 | 4.7 |
| 34 | 70.5 | 43.9 | 15.6 | 4.5 |
| 35 | 73.0 | 48.1 | 15.5 | 4.7 |
| 36 | 83.1 | 54.8 | 19.6 | 4.2 |
| 37 | 89.0 | 55.3 | 19.9 | 4.5 |
| 38 | 76.5 | 61.4 | 21.9 | 3.5 |
| 39 | 49.6 | 22.3 | | |
| 40 | 48.8 | 30.1 | | |
| 41 | 55.3 | 35.6 | | |
| 42 | 39.4 | 38.9 | | |
| 43 | 52.5 | 43.5 | | |
| 44 | 65.9 | 31.8 | 26.8 | 2.5 |
| 45 | 61.7 | 37.6 | 28.5 | 2.2 |
| 46 | | 35.9 | | |
| 47 | | 21.6 | | |
| 48 | | 20.7 | | |
| 49 | 25.4 | 24.4 | | |
| 50 | 31.3 | 30.1 | | |
| 51 | 33.3 | 25.0 | | |
| 52 | 36.6 | 25.4 | | |
| 53 | 63.0 | 40.5 | 32.1 | 2.0 |
| 54 | 57.2 | 43.7 | 30.4 | 1.9 |
| 55 | 63.9 | 44.7 | 30.2 | 2.1 |
| 56 | 55.9 | 52.5 | 36.2 | 1.5 |

(continued)

(continued)

| Lirae space number | Ventral (V) | Midflank | Dorsal (D) | Ratio V/D |
|---|---|---|---|---|
| 57 | 70.3 | 56.0 | 43.8 | 1.6 |
| 58 | 66.1 | 57.9 | 50.2 | 1.3 |
| 59 | 53.4 | 51.2 | 42.9 | |
| 60 | 64.5 | 44.2 | | |
| 61 | 53.5 | 40.6 | | |
| 62 | 68.7 | 47.0 | | |
| 63 | 51.3 | | | |
| 64 | 52.0 | | | |
| 65 | 26.5 | | | |

# Appendix 11

Lirae spacing (in microns) on the embryonic shell of *Fidelites fidelis* (AMNH 50417).

| Lirae Space number | Ventral (V) | Midflank | Dorsal (D) | Ratio V/D |
|---|---|---|---|---|
| 1 | 15.2 | | | |
| 2 | 25.5 | | | |
| 3 | 33.7 | | 29.9 | 1.1 |
| 4 | 47.9 | | 30.7 | 1.6 |
| 5 | 45.3 | | | |
| 6 | 44.1 | | | |
| 7 | 44.1 | 42.7 | | |
| 8 | 50.9 | 39.4 | | |
| 9 | 45.3 | | | |
| 10 | 42.8 | 28.9 | | |
| 11 | 46.2 | 27.4 | | |
| 12 | 45.0 | 29.3 | 16.9 | 2.7 |
| 13 | 48.5 | 30.6 | 18.4 | 2.6 |
| 14 | 46.9 | 30.8 | 21.6 | 2.2 |
| 15 | 48.2 | 32.4 | 19.6 | 2.5 |
| 16 | 52.7 | 38.8 | 16.8 | 3.1 |
| 17 | 43.6 | 31.5 | 14.2 | 3.1 |
| 18 | 56.0 | 41.4 | 18.4 | 3.0 |
| 19 | 61.2 | 37.4 | 13.3 | 4.6 |
| 20 | 62.3 | 42.9 | 19.9 | 3.1 |
| 21 | 61.4 | 37.7 | 17.1 | 3.6 |
| 22 | 57.3 | 32.9 | 14.6 | 3.9 |
| 23 | 60.7 | 42.3 | 15.7 | 3.9 |
| 24 | 62.6 | 42.3 | 20.0 | 3.1 |
| 25 | 72.4 | 47.2 | | |
| 26 | 89.0 | 57.4 | | |
| 27 | 71.7 | 50.8 | | |

(continued)

(continued)

| Lirae space number | Ventral (V) | Midflank | Dorsal (D) | Ratio V/D |
|---|---|---|---|---|
| 28 | | 62.0 | | |
| 29 | 85.0 | 58.0 | | |
| 30 | 95.4 | 65.5 | | |
| 31 | 92.0 | 62.0 | | |
| 32 | 91.1 | 66.0 | | |
| 33 | 107.3 | 72.8 | | |
| 34 | 99.2 | 73.4 | | |
| 35 | 97.6 | 67.6 | | |
| 36 | 89.1 | 74.6 | | |
| 37 | 86.6 | 72.6 | | |
| 38 | 137.6 | 73.1 | | |
| 39 | 202.0 | 126.4 | | |
| 40 | 210.4 | 120.3 | | |
| 41 | 134.1 | 107.0 | 84.8 | 1.6 |
| 42 | 123.5 | 93.5 | 74.2 | 1.7 |
| 43 | 156.6 | | | |

## References


Arnold, J. M., N. H. Landman, and H. Mutvei. 1987. Development of the embryonic shell of *Nautilus. In* W. B. Saunders, and N. H. Landman (editors), *Nautilus – the Biology and Paleobiology of a Living Fossil*, pp. 373–400. New York: Plenum Press.

Bandel, K. 1982. Morphologie und Bildung der früh ontogenetischen Gehäuse bei conchiferen Mollusken. *Facies* **7**: 1–198.

Bandel, K. 1986. The ammonitella: a model of formation with the aid of the embryonic shell of archaeogastropods. *Lethaia* **19**: 171–180.

Barrande, J. 1865. Systême Silurien du centre de la Bohême. I. Vol. II. Céphalopodes. Praha and Paris.

Becker, R. T., and M. R. House. 1994. International Devonian goniatite zonation, Emsian to Givetian, with new records from Morocco. *Courier Forschungs-institut Senckenberg, Frankfurt am Main* **169**: 79–135.

Becker, R. T., and J. Kullmann. 1996. Paleozoic ammonoids in space and time. *In* N. H. Landman, K. Tanabe, and R. A. Davis (editors), *Ammonoid Paleobiology*, pp. 711–753. New York: Plenum Press.

Bensaïd, M. 1974. Étude sur des Goniatites à la limite du Dévonien moyen et supérieur du Sud marocain. *Notes du Service Géologique du Maroc* **36**(264): 81–140.

Berthold, T., and T. Engeser. 1987. Phylogenetic analysis and systematization of the Cephalopoda (Mollusca). *Verhandlungen Naturwissenscaftlichen vereins in Hamburg* (*NF*) **29**: 187–220.

Branco, W. 1879–80. Beiträge zur Entwicklungsgeschichte der fossilen Cephalopoden, Theile I. *Palaeontographica* **26**: 19–50, pls. 4–13.

Branco, W. 1880–81. Beiträge zur Entwicklungensgeschichte der fossilen Cephalopoden, Theile II. *Palaeontographica* **27**: 17–81, pls. 3–17.

Bogoslovsky, B. I. 1969. Devonskie Ammonoidei. I. Agoniatity. *Trudy Paleontologicheskogo Institita Akademiya Nauk SSSR* **124**: 341pp.

Bucher, H., N. H. Landman, S. M. Klofak, and J. Guex. 1996. Modes and rate of growth in ammonoids. *In* N. H. Landman, K. Tanabe, and R. A. Davis (editors), *Ammonoid Paleobiology*, pp. 407–461. New York: Plenum Press.

Bucher, H., R. Chirat, and J. Guex. 2003. Morphogenetic origin of radial lirae and mode of shell growth in *Calliphylloceras* (Jurassic Ammonoidea). *Eclogae geologicae Helvetiae* **96**: 495–502.

Checa, A. 1995. A model for the morphogenesis of ribs in ammonites inferred from associated microsculptures. *Palaeontology* **37**: 863–888.

Chirat, R., and S. v. Boletzky. 2003. Morphogenetic significance of the conchal furrow in nautiloids: evidence from early embryonic shell development of Jurassic Nautilida. *Lethaia* **36**: 161–170.

Chlupáč, I., and V. Turek. 1983. Devonian goniatites from the Barrandian area, Czechoslovakia. *Edice Rozpravy Ustrední_hoústavu geologického*, *svazek* **46**: 159pp. [Translated by I. Chlupáčand H. Zárubová]

Clarke, J. M. 1899. Notes on the early stages of certain goniatites. *Annual Report of the New York State Geologist 16* (*Annual Report of the New York State Museum*) **50**(2): 163–169.

Clausen, C. D. 1969. Oberdevonische Cephalopoden aus dem Rheinischen Schiefergebirge, II Gephuroceratidae, Beloceratidae. *Palaeontographica Abteilungen A* **132**: 95–178.

Doguzhaeva, L. A. 1996a. Microstructure of juvenile shells of the Permian *Hemibactrites* sp. (Cephalopoda: Bactritoidea). *Doklady Biological Sciences* **349**(2): 275–279.

Doguzhaeva, L. A. 1996b. Shell ultrastructure of the early Permian bactritella and ammonitella, and its phylogenetic implication. *Jost Wiedmann Symposium. Cretaceous Stratigraphy, Paleobiogeology and Paleobiogeography Abstracts*, pp. 19–25.

Doguzhaeva, L. A. 2002. Adolescent bactritoid, orthoceroid, ammonoid and coleoid shells from the upper Carboniferous and lower Permian of the South Urals. *In* H. Summesberger, K. Histon, and A. Daurer (editors), *Cephalopods – Present and Past. Abhandlungen Geologische Bundesanstalt* **57**: 9–55.

Drushschits, V. V., L. A. Doguzhayeva, and I. A. Mikhaylova. 1977. The structure of the ammonitella and the direct development of ammonites. *Paleontological Journal* **2**: 57–69.

Engeser, T. 1990. Major events in cephalopod evolution. *In* P. D. Taylor, and G. P. Larwood (editors), *Major Evolutionary Radiations. Systematics Association Special Volume* **42**: 119–138, Oxford: Clarendon Press.

Engeser, T. 1996. The position of the Ammonoidea within the Cephalopoda. *In* N. H. Landman, K. Tanabe, and R. A. Davis (editors), *Ammonoid Paleobiology*, pp. 3–19. New York: Plenum Press.

Erben, H. K. 1950. Bemerkungen zu Anomalien mancher Anfangswindungen von *Mimagoniatites fecundus* (Barr.) *Neues Jahrbuch für Geologie und Paläontologie*, *Monathefte*, pp. 25–32.

Erben, H. K. 1953. Goniatitacea (Ceph.) aus dem Unterdevon und Unterem Mitteldevon. *Neues Jahrbuch für Geologie und Paläontologie Abhandlungen* **98**: 175–225.

Erben, H. K. 1960. Primitive Ammonoidea aus dem Unterdevon Frankreichs und Deutschlands. *Neues Jahrbuch für Geologie und Paläontologie Abhandlungen* **110**(1): 1–128.

Erben, H. K. 1962. Über böhmische und türkische Vertreter von *Anetoceras* (Ammon., Unterdevon). *Paläontologische Zeitschrift* **36**(1/2): 14–27.

Erben, H. K. 1964a. Bactritoidea. *In* R. C. Moore (editor), *Treatise on Invertebrate Paleontology*, *Part K*, *Mollusca 4*, *Cephalopoda*: *K491–505*. Lawrence, Kansas, and New York: The University of Kansas Press and the Geological Society of America.

Erben, H. K. 1964b. Die Evolution der ältesten Ammonoidea, Lieferung 1. *Neues Jahrbuch für Mineralogie*, *Geologie*, *Paläontologie Abhandlungen* **120**(2): 107–212.

Erben, H. K. 1965. Die Evolution der ältesten Ammonoidea (Lieferung II). *Neues Jahrbuch für Mineralogie*, *Geologie Paläontologie Abhandlungen* **122**(3): 275–313.

Erben, H. K. 1966. Über den Ursprung der Ammonoidea. *Biological Review* **41**: 641–658.

Erben, H. K., G. Flajs, and A. Siehl 1968. Ammonoids: early ontogeny of ultramicroscopical shell structure. *Nature* **219**(5152): 396–398.

Göddertz, B. 1987. Devonische Goniatiten aus SW-Algerien und ihre stratigraphische Einordnung in die conodonten-Abfolge. *Palaeontographica Abteilung A* **197**: 127–220.

Göddertz, B. 1989. Unterdevonische Hercynische Goniatiten aus Deutschland, Frankreich und der Türkei. *Palaeontographica Abteilungen A* **208**(1–3): 61–89.

House, M. R. 1962. Observations on the ammonoid succession of the North American Devonian. *Journal of Paleontology* **36**(2): 247–284.

House, M. R. 1965. A Study on the Tornoceratidae: the succession of *Tornoceras* and related genera in the North American Devonian. *Philosophical Transactions of the Royal Society London Series B* **250**: 79–130.

House, M. R. 1981. On the origin, classification and evolution of the early Ammonoidea. *In* M. R. House, and J. R. Senior (editors), *The Ammonoidea. Systematic Association Special Volume* **18**: 3–36, New York: Academic Press.

House, M. R. 1996. Juvenile goniatite survival strategies following Devonian extinction events. *In* M. B. Hart (editor), *Biotic Recovery from Mass Extinction Events. Geological Society Special Publication* **102**: 163–185.

Hyatt, A. 1883. Fossil cephalopods in the Museum of Comparative Zoology. *American Association for the Advancement of Science Proceedings* **32**: 323–361.

Jacobs, D. K., and N. H. Landman. 1993. *Nautilus* – a poor model for the function and behavior of ammonoids? *Lethaia* **26**: 101–111.

Klofak, S. M., N. H. Landman, and R. H. Mapes. 1999. Embryonic development of primitive ammonoids and the monophyly of the Ammonoidea. *In* F. Oloriz, and F. J. Rodriguez-Tovar (editors), *Advancing Research on Living and Fossil Cephalopods*, pp. 23–45. New York: Plenum Press.

Klug, C. 2001. Early Emsian ammonoids from the eastern Anti-Atlas (Morocco) and their succession. *Paläontologische Zeitschrift* **74**(4): 479–515.

Klug, C., D. Korn, and A. Reisdorf. 2000. Ammonoid and conodont stratigraphy of the late Emsian to early Eifelian (Devonian) at the Jebel Ouaoufilal (near Taouz, Tafilalt, Morocco). *Travaux de l'Institut Scientifique*, *Rabat*, *Série Géologie et Géographie Physique* **20**: 45–56.

Korn, D. 2001. Morphometric evolution and phylogeny of Palaeozoic ammonoids. Early and Middle Devonian. *Acta Geologica Polonica* **5**(3): 193–215.

Korn D., and C. Klug. 2002. Ammoneae Devonicae. *In* W. Riegraf (editor), *Fossilium Catalogus 1*: *Animalia* **138**: 1–375, Leiden: Backhuys.

Kulicki, C. 1974. Remarks on the embryogeny and postembryonal development of ammonites. *Acta Palaeontologica Polonica* **19**(2): 201–224.

Kulicki, C. 1979. The ammonite shell: its structure, development and biological significance. *Palaeontologia Polonica* **39**: 96–141.

Landman, N. H. 1988. Heterochrony in ammonites. *In* M. L. McKinney (editor), *Heterochrony in Evolution*, *pp*. 159–182. New York: Plenum Press.

Landman, N. H., K. Tanabe, and Y. Shigeta. 1996. Ammonoid embryonic development. *In* N. H. Landman, K. Tanabe, and R. A. Davis (editors), *Ammonoid Paleobiology*, *pp*. 343–405. New York: Plenum Press.

Landman, N. H., F. Bizzarini, K. Tanabe, R. H. Mapes, and C. Kulicki. 2001. Micro-ornament on the embryonic shells of Triassic ceratites (Ammonoidea). *American Malacological Bulletin* **16**(1/2): 1–12.

Mapes, R. H. 1979. Carboniferous and Permian Bactritoidea (Cephalopoda) in North America. *The University of Kansas Paleontological Contributions Article* **64**: 1–75.

Miller, A. K. 1938. Devonian ammonoids of America. *Geological Society of America Special Papers Number* **14**: 262pp.

Miller, A. K., and W. M. Furnish. 1954. The classification of the Paleozoic ammonoids. *Journal of Paleontology* **28**(5): 685–692.

Owen, C. B. 1878. On the relative positions to their constructors of the chambered shells of Cephalopods. *Proceedings of the Zoological Society of London* **1878**: 955–975.

Petter, G. 1959. Goniatites Dévoniennes du Sahara. *Publications du Service de la Carte Géologique de l'Algérie* (*Nouvelle Séries*) *Paléontologie Mémoire* **2**: 313pp.

Ristedt, H., 1968. Zur Revision der Orthoceratidae. *Akademie der Wissenschaften und der Literatur Mainz Abhandlungen der Mathematisch-Naturwissenschaftlichen Klasse* **1968**: 211–287.

Ruzhentsev, V. E. 1960. Printsipy sistematiki, sistema i filogeniya paleozoyskikh ammonoidey. *Trudy Paleontologicheskogo Instituta Akademiya Nauk SSSR* **83**: 331pp. [Principles of systematics, classification and phylogeny of Paleozoic ammonoids].

Ruzhentsev, V. E. 1974. Suborder Ammonoidea; general section. *In* V. E. Ruzhentsev (editor), *Fundamentals of Paleontology, Mollusca-Cephalopoda I* **5**: 371–503. Jerusalem: Kater Publishing House. [Translated by Israel Program for Scientific Translation].

Sandberger, G. 1851. Beobachtungen über mehrere schwierige Puncte der Organisation der Goniatiten. *Jahrbücher des Vereins für Naturkunde im Herzogthum Nassau* **7**: 292–304.

Schimansky, V. N. 1954. Pryamye nautiloidei i baktritoidei sakmarskogo artinskogo yarusov Yuzhnogo Urala (Straight nautiloids and bactritoids from the Sakmarian and Artinskian stages of the southern Urals). *Trudy Paleontologicheskii Institut Akademiia Nauk SSSR* **44**: 1–156.

Schindewolf, O. H. 1933. Vergleichende Morphologie und Phylogenie der Anfangskammern tetrabrachiater Cephalopoden – eine Studie über Herkunft, Stammesentwicklung und System der niederen Ammonoideen. *Abhandlungen preussischen Geologischen Landesanstalt, Berlin. Neue folge* **148**: 1–115.

Sprey, A. 2002. Tuberculate micro-ornament on the juvenile shell of Middle Jurassic ammonoids. *Lethaia* **34**: 31–35.

Tanabe, K. 1989. Endocochliate embryo model in the Mesozoic Ammonitida. *Historical Biology* **2**: 183–196.

Tanabe, K., N. H. Landman, and R. H. Mapes. 1994. Early shell features of some Late Paleozoic ammonoids and their systematic implications. *Transactions and Proceedings of the Palaeontological Society of Japan*, *New Series* **173**: 384–400.

Tanabe, K., J. Tsukahara, Y. Fukuda, and Y. Fukada. 1991. Histology of a living *Nautilus* embryo: preliminary observations. *Journal of Cephalopod Biology* **2**(1): 13–22.

Vermeij, G. J. 1993. *A Natural History of Sea Shells*. Princeton, New Jersey: Princeton University Press.

Wissner, U. F. G., and A. W. Norris. 1991. Middle Devonian goniatites from the Dunedin and Besa River Formations of Northeastern British Columbia. *Contributions to Paleontology*, *Geological Survey of Canada Bulletin* **412**: 45–79.